Effect of Synthetic Marrow on Synthetic Open-Cell Foam Vertebrae

BY

Brian Victor Good

Submitted to the graduate degree program in Bioengineering and the Graduate Faculty of the University of Kansas in partial fulfillment of the requirements for the degree of Master of Science.

_____
Dr. Elizabeth A. Friis, Chairperson

_____
Dr. Sara Wilson, Committee Member

_____
Dr. Terry Faddis, Committee Member

Date Defended: _____

The Thesis Committee for Brian Victor Good certifies that this is the approved version of the following thesis:

Effect of Synthetic Marrow on Synthetic Open-Cell Foam Vertebrae

_____

Dr. Elizabeth A. Friis, Chairperson

_____

Dr. Sara Wilson, Committee Member

_____

Dr. Terry Faddis, Committee Member

Date approved:_____

Acknowledgments

There are several people I would like to thank for their contributions to my success:

- Dr. Elizabeth Friis for her continual support, guidance, and confidence. Dr. Friis was the guiding force behind my perseverance. Beyond the obvious help and instruction, her understanding and commitment to me and my work made this feat possible. I am more grateful to Dr. Friis than I could ever describe.

- Dr. Sara Wilson and Dr. Terry Faddis for serving on my committee and for the background of knowledge they imparted in previous coursework.

- The Departments of Bioengineering and Mechanical Engineering have been cornerstones in my development and education. My time spent at the University of Kansas in these departments has been filled with nothing but pleasant and positive interactions with both faculty and staff.

- Washburn University for their contribution to my education. I would especially like to thank Dr. Keith Mazachek for his direction in my undergraduate years at Washburn and continued support throughout graduate school.

- John Domann for his patience and understanding. John was my go-to person when I needed help, advice, or support in the lab. I will be forever indebted.

- Members of our lab including, but not limited to, Erin Lewis, Damon Mar, Nikki Johnson, and Nick Tobaben for their insight, assistance, and high spirits.

- Charles Gabel for his help and wisdom in the machine shop. Charles spent some of his valuable time machining the jigs used in the testing.

- John James and Amy Johnson for their work on the producing and providing the specimens for testing.

- My parents Donald and Margery Good and my sisters Dr. Kari Harris and Kristina Wagner for their continued love and support throughout my education. I wouldn't and couldn't be where I am today without them.

- Jon Davis, Tom Devlin, and Katie Risley for their encouragement, understanding, and assistance countless ways.

- There were so many more people that have had significant contributions to my success. I want to thank all of you – you know who you are. You have made the last few years enjoyable and successful.

Abstract

The intended purpose of this research is to further supplement the first generation of the Analogue Spine Model (ASM) by introducing a bone marrow component. Currently the ASM does not include a bone marrow component. While not mechanically relevant, bone marrow does have an effect on bone cement intrusion. Techniques such as brushing (removing surface debris) and pressurized lavage (removing marrow from bone interstices) used in preparation for the bone-cement interface during surgical procedures have been shown to improve cement intrusion into the cancellous bone. This indicates that marrow may play a key role in bone cements' contribution to anchoring bone screws. The addition of a bone marrow component to the analogue spine model will create a more realistic testing platform for medical devices employing bone screws. Preliminary work has identified glycerin as a candidate for use as a yellow marrow substitute due to its viscosity and availability.

Four point bending was utilized as a rapid, preliminary assessment of the synthetic marrow's effect on the resins used to produce cancellous and cortical bone. Specimens produced by Pacific Research Laboratories (PRL) were soaked in the synthetic marrow for durations of two and four weeks and compared to a control group. Results showed significant difference between the groups in modulus and ultimate stress.

Synthetic marrow's effect on analogue cancellous bone was then assessed by compression testing and bone screw pullout testing. Specimens produced by PRL were soaked for four weeks in the synthetic marrow and compared to a control. Modulus, yield stress, ultimate stress, and pullout strength were all found to be significantly decreased by the synthetic marrow.

The change in material properties was significant in terms of statistics; however, values for these properties were still in the range of reported literature values. Further testing is necessary to ensure properties do not continue to decrease in longer soaking durations.

Table of Contents

List of Figures

List of Tables

List of Symbols

R – rate of crosshead motion (mm/min)

Z – rate of straining of the outer fibers (shall equal 0.01 mm/mm per ASTM Standard)

L – support span (mm)

d – depth of beam (mm)

σ – maximum stress of specimen (MPa)

P – load at a given point on the load-deflection curve (N)

b – width of beam (mm)

ε – maximum stress of specimen (mm/mm)

D – maximum deflection of center of beam (mm)

E – modulus of elasticity in bending (MPa)

m – slope of tangent to the initial straight-line

List of Abbreviations

ASM: Analogue Spine Model

PRL: Pacific Research Laboratories

NIH: National Institute of Health

ALL: Anterior longitudinal ligament

PLL: Posterior longitudinal ligament

IVD: Intervertebral disc

id: inner diameter

od: outer diameter

TPI: threads per inch

Preface

The format of this thesis is designed to alleviate the burden of publication of the material presented. This thesis initially follows a classic format, and then it deviates in Chapters 2 and 3, which are designed to be pulled directly from the thesis for publication with only minor changes. This format allows for faster publication, which benefits the researchers, faculty, department, and ultimately the university.

Chapter 1: Introduction & Significance

The intended purpose of this research is to further supplement the first generation of the Analogue Spine Model (ASM) by introducing a bone marrow component. In order to accomplish this, two key tasks need to be addressed. First, a material must be selected that has similar rheological qualities as human bone marrow, and second, the material must not degrade or alter the mechanical properties of the existing synthetic trabecular bone.

This work is being completed to further the current model by making it more realistic for use in research applications such as bone cement intrusion, vertebroplasty, and kyphoplasty studies, and to a much lesser extent model the hydrostatic pressure within the vertebral body. The following is a discussion on the background of the human spine and its components, the current spine models, and the need for this research to be incorporated into the ASM.

1.1 Spinal Anatomy Overview

The adult human spine is comprised of 24 individual vertebrae and eight to ten fused bones in the sacral/coccygeal regions [1]. There are two main components of the vertebrae, as shown in Figure 1: the vertebral body or centrum, which is the main load bearing unit of the spine, and the posterior elements which have numerous ligament and tendon attachment sites and articulate with the superior and inferior vertebrae. Vertebrae contain two different types of bone tissue. The outer shell of the vertebrae consists of dense cortical bone, and contained by this shell is porous cancellous (or trabecular) bone.

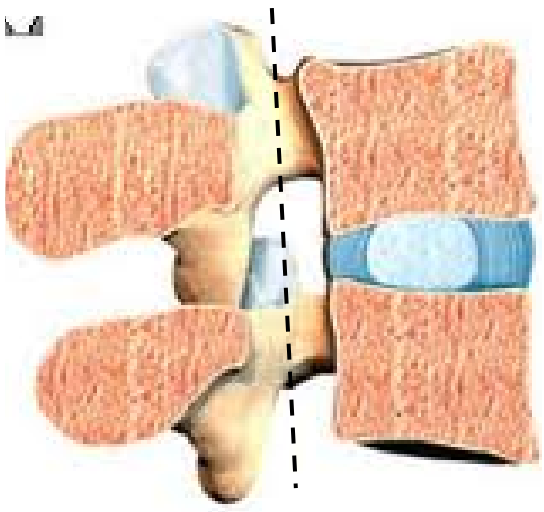

***Figure 1: Two vertebrae as seen in the sagittal plane. To the right of the dashed line are the centrum; to the left are the posterior elements. Reproduced from http://harms-spinesurgery.com with permission* [76].**

Cancellous bone is comprised of many individual micro-struts or trabeculae, which create an interconnected, open-celled structure that is filled with bone marrow and other cells *in vivo* [2]. The following is a more detailed description of the components of the vertebrae.

1.2 Cortical Bone

As mentioned, the vertebra has a very thin, dense shell of compact cortical bone ranging in thickness from 0.11 to 1.94 mm (means reported 0.40 – 0.68 mm) [3-4]. The basic functional unit of cortical bone is the osteon, which consists of concentric layers of osteocytes. Osteocytes form around a central canal which contains the blood vessels that supply the osteon with nutrients. These concentric rings of osteocytes around the central canal (Haversian canal) resemble a "bull's-eye" when viewing a cross section. Central

canals are normally aligned parallel to the normal loading axis of the bone. Perforating canals (Volkmann canals) are aligned perpendicular to the surface of the bone and supply nutrients to deep osteons and service the bone marrow located within the bone.

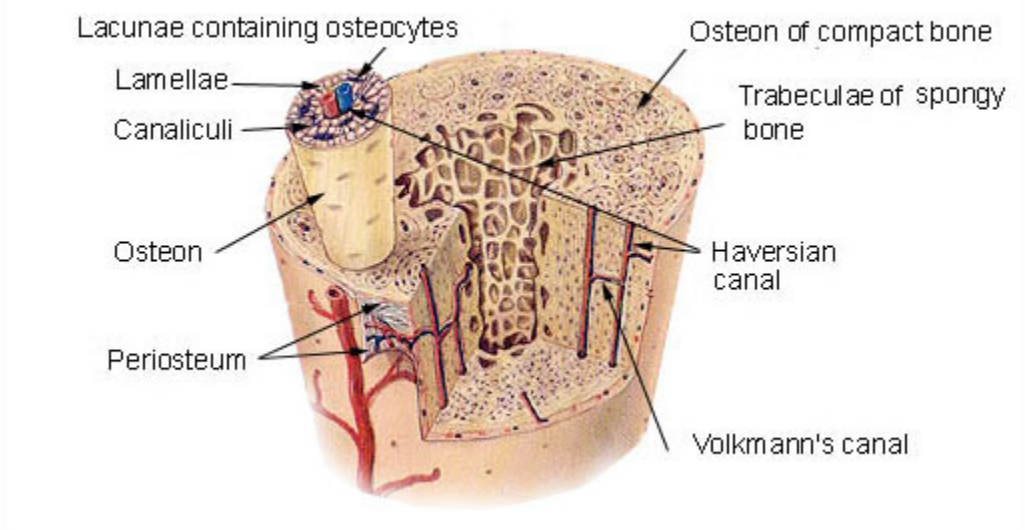

Figure 2: General schematic of cortical bone. Reprinted with permission from http://training.seer.cancer.gov/ **[5]**

The thickness of the cortical shell in the lumbar region typically ranges from 0.27 to 0.38 mm [6-8]. The shell is thin when comparing it to vertebral cross-sectional width, which is in the range of 34 mm [9]. Even though the shell is thin, its bone mass fraction (mass of shell / mass of vertebrae) has been found to be in the range of 0.21 – 0.29 [6], demonstrating the density of the cortical shell; therefore, its mechanical contribution could be relevant.

Many studies have been conducted to attempt to estimate the cortical shell's compressive strength contribution to the vertebral bodies. These estimates vary greatly, ranging from 10 -75%, however, many of these studies use different methods of testing,

both numerical and biomechanical, and boundary conditions used in these tests have also varied [6, 10-12]. More reliable studies report the strength contribution of the cortical shell to the vertebral body is less than 15% [13].

1.3 Cancellous Bone

Cancellous bone is found within the cortical shell of the vertebrae. It is composed of rod and plate-like structures known as trabeculae. The trabeculae form an interconnected, three dimensional network that give a spongy, honeycomb appearance, closely resembling an open-cell cellular solid (Figure 3).

***Figure 3: Micro-scale image of human trabecular bone from the iliac crest showing the honeycomb appearance. Reprinted with permission from http://www.scielo.br/* [14].**

1.3.1 Mechanical Function

The bulk of each vertebrae's strength can be attributed to cancellous bone, and it is the key hard tissue responsible for energy absorption [15]. The appearance and mechanical properties of cancellous bone are highly dependent on several conditions including anatomical site [16]. It has been shown that trabeculae form along the axis of principle stress [17] and have the ability to remodel and functionally adapt to mechanical loads over time (generally referred to as Wolff's law) [16]. Thus, in the centrum of the vertebrae near the endplates, where forces are primarily axially compressive, the cancellous bone is denser; the trabeculae are rod-like in appearance and orientated axially [13, 16]. Near the center of the vertebrae, the cancellous bone is less dense and the trabeculae are more plate-like in structure [13].

1.3.2 Factors Affecting Quality

Age, gender, and activity level also influence the structure of cancellous bone as shown in Figure 4. Younger cancellous bone is typically composed of rigid, plate-like structures with a relatively high amount of cross-linking by rod-shaped trabeculae. As the bone ages, the plate-like structures lose thickness and gaps are produced through continuous tissue remodeling [13]. In addition, the amount of cross-linking, rod-like structures slowly decreases giving the bone an even more open-celled look. These changes can cause a significant decrease in mechanical properties due to the reduced number of trabeculae in the bone as shown in Figure 4.

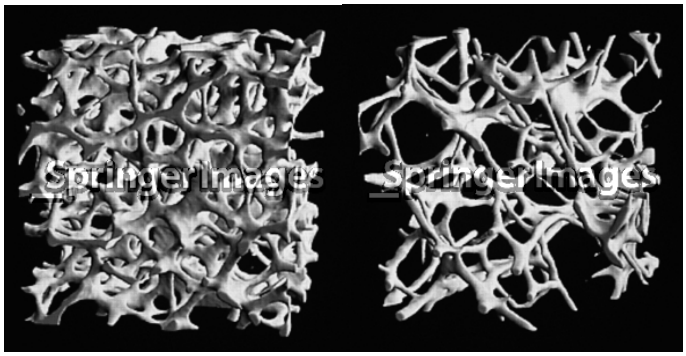

Figure 4: Age and gender-related differences in vertebral trabecular bone. a.) A 42 year-old male and b.) an 84 year-old woman. Reprinted with permission from Springer Images **[18].**

In addition to the mechanical role of stabilization and support, cancellous bone is also involved in metabolic functions. Cancellous bone plays a vital role in mineral storage and maintaining mineral homeostasis within the human body. It is capable of storing or dispersing minerals, most notably, calcium and phosphate, as needed [19]. In addition, bone has been shown to retain 95% of the body's sodium and 50% of its magnesium. These minerals play a critical role in other chemical reactions in the body including regulation of extracellular fluid, neuromuscular activity, blood clotting, and intracellular signal transduction. Storage of these minerals is a significant factor in the structural integrity of the vertebrae. Cancellous bone has a high surface to volume ratio and is highly vascularized; consequently, it is susceptible to metabolic alterations. Metabolic conditions such as osteoporosis can flush mineral stores and limit the body's ability to store minerals, thus causing a significant decrease in density and strength (Figure 5). Cancellous bone is

also the body's second line of defense against acidosis and is also capable of absorbing toxins and heavy metals limiting their adverse effects [19].

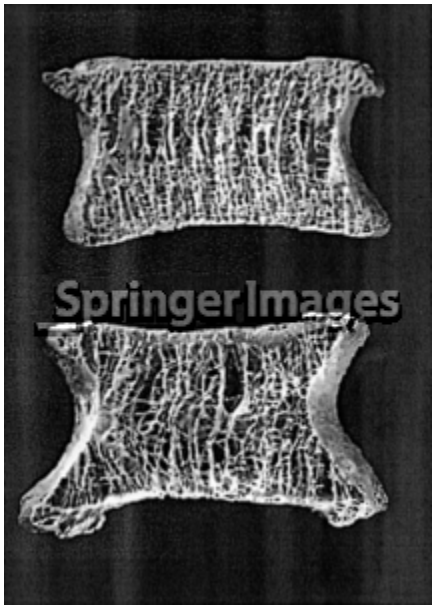

***Figure 5: Metabolic changes - normal (top) and osteoporotic (bottom) vertebral bodies. Reprinted with permission from Springer Images* [77].**

As mentioned, cancellous bone is capable of these metabolic functions due to its high surface to volume ratio and immediate interface with hematopoietic (red) bone marrow contained within the vertebrae. Thus, the microenvironment surrounding cancellous bone is the site of formation of new red blood cells from the stem-cell line inherent to the hematopoietic bone marrow [20].

1.4 Bone Marrow

Bone marrow resides within the cortical shell and throughout the cancellous core. In addition to the red marrow, which mainly consists of hematopoietic cells, yellow marrow (mainly consisting of fat) is also found within the vertebrae. Another cellular component of marrow is a highly organized stroma that acts as scaffolding to support the proliferation of the hematopoietic cells [21]. At birth, all bone marrow is red marrow. As we age, red marrow is converted to yellow marrow. Relative fat content of marrow has been shown to increase from 23.9% in subjects from ages 11-20 to 54.2% in subjects 61 years or older [8]. Also, females have a lower relative fat content of marrow in all age ranges [8]. In addition, fat content of marrow is increased in subjects suffering from osteoporosis or osteopenia [22].

While bone marrow plays a primary role in the metabolic functions of the vertebrae, it has been shown that it does not significantly strengthen or stiffen the vertebrae at physiological strain rates. At high strain rates, such as high impact trauma situations, vertebrae can be hydraulically stiffened and strengthened by the fluid flow of marrow [23] [24-25]. Normal intermedullary pressure is around 30 mmHg, approximately one-fourth the normal blood pressure (110 – 140 mmHg); this is commonly referred to as the one-fourth rule [26, 22]. The marrow cavity is quite susceptible to external factors which have been shown to raise or lower the intermedullary cavity pressure, mainly due to hemodynamic changes. These factors include normal physiological loading, such as exercise, occlusion of regional vessels, and prescription injections, such as epinephrine and norepinephrine [21].

There is limited data on the rheological properties of human bone marrow. The only study found showed that the viscosity of human bone marrow was on average 37.5 cP at 36°C. The study also found that the marrow (predominately yellow marrow) behaved as a Newtonian fluid, whereas strictly red marrow behaves as non-Newtonian fluid [27]. This is plausible because red marrow has a higher concentration of red blood cells, and it has been well documented that blood behaves as a non-Newtonian fluid [27]. In addition, the density of red marrow (1.06 g/cm^3) [35] is close to that of blood (1.05 g/cm^3) [28]. There have been limited studies on the density of yellow marrow. However, those that have been published show that yellow marrow (fatty marrow) has a density of 0.89 g/cm^3 [29], which is comparable to the density of fatty tissue (0.92 g/cm^3) [30]. It should also be noted that in bovine specimens, different anatomical locations of marrow samples yielded different viscosities which has been mainly attributed to locations of red and yellow marrow, but also due to experimental methods [29].

1.5 Current Spine Models

The above mentioned factors, among others, are responsible for a large amount of variability in human cancellous bone. Vertebral cancellous bone has been found to have moduli ranging from 100 to 700 MPa, and some estimate an even larger range (10 - 3000 MPa) for locations not limited to the vertebral cancellous bone [15, 31-32]. Many of these studies use compression as the mode of testing and have not accounted for a significant source of variation, which may arise if the ends of the test specimens are placed in direct contact with the loading platens. This occurs due to frictional forces acting on individual

free struts (end artifacts) of the bone, and previous research shows this causes an overestimate the modulus and yield strain of human trabecular bone by 40% [33]. More recent studies which have capped the ends of the test specimens, have found the modulus of vertebral cancellous bone to be in the range of 290 – 350 MPa [34-35]. Capping specimen ends entails embedding the free struts of the ends of the bone specimen in a hardening putty such as poly(methyl methacrylate) or Bondo™ (3M™; St. Paul, MN). Table 1 summarizes these findings.

Table 1: Literature values for the moduli of vertebral cancellous bone. All values were tested in the longitudinal direction.

Author	Year	Boundary Condition	Avg	Std Dev	Min	Max
Banse [35]	2002	Capped	352	145	127	725
Morgan / Keaveny [36]	2002	Capped	344	148	---	---
Kopperdahl / Keaveny [34]	1998	Capped	291	113	90	536
Moseklide [37]	1987	Platen	67	7	---	---
Hou [32]	1998	Platen	316	226	10.6	975.6
Lindahl [38]	1976	Platen	55.6	0.7	1.1	139

Yield stress values for vertebral cancellous bone range from approximately 2 – 4 MPa (Table 2) [34, 36, 38]. Generally a 0.2% offset method common to other engineering

materials is used to find the yield stress. Yield strain is the strain found at the point of yield stress and varies greatly depending on the test set-up. Un-capped specimens generally give a higher value for yield strain as can be seen when comparing the studies in Table 3 [34, 36, 38].

Table 2: Literature values for the yield stress of vertebral cancellous bone.

Author	Year	Boundary Condition	Avg	Std Dev	Min	Max
Morgan / Keaveny [36]	2002	Capped	2.02	0.92	---	---
Kopperdahl / Keaveny [34]	1998	Capped	1.92	0.84	0.56	3.71
Lindahl [38]	1976	Platen	4	0.1	0.1	9.7

Table 3: Literature values for the yield strain of vertebral cancellous bone.

Author	Year	Boundary Condition	Avg	Std Dev	Min	Max
Morgan / Keaveny [36]	2002	Capped	0.77 %	0.06 %	---	---
Kopperdahl / Keaveny [34]	1998	Capped	0.84 %	0.06 %	0.75 %	0.95 %
Lindahl [38]	1976	Platen	6.7 %	0.2 %	4.1 %	8.60 %

Table 4 shows the ultimate stress of vertebral cancellous bone ranges from approximately 2 – 5 MPa (Table 4) [34, 36, 38]. This property is defined as the maximum stress achieved. Ultimate strain is the strain at the point of ultimate stress and ranges from

about 1 – 10% [34, 35, 37, 38]. Ultimate strain is highly dependent on the boundary conditions of the test set-up. Much higher values for ultimate strain are found in studies with un-capped boundary conditions as can be seen in Table 5 [37, 38].

Table 4: Literature values for the ultimate stress of vertebral cancellous bone.

Author	Year	Boundary Condition	Avg	Std Dev	Min	Max
Banse [35]	2002	Capped	2.37	1.14	0.6	6.17
Kopperdahl / Keaveny [34]	1998	Capped	2.23	0.95	0.7	4.33
Moseklide [37]	1987	Platen	2.45	0.24	---	---
Hou [32]	1998	Platen	3.29	2.34	---	---
Lindahl [38]	1976	Platen	4.6	0.3	0.2	10.5

Table 5: Literature values for the ultimate strain of vertebral cancellous bone.

Author	Year	Boundary Condition	Avg	Std Dev	Min	Max
Banse [35]	2002	Capped	1.19 %	0.26 %	0.72 %	2.01 %
Kopperdahl / Keaveny [34]	1998	Capped	1.45 %	0.33 %	0.96 %	2.30 %
Moseklide [37]	1987	Platen	7.40 %	0.20 %	---	---
Lindahl [38]	1976	Platen	9.50 %	0.40 %	5.30 %	1.44 %

Variability is not restricted to cancellous bone; large variations have been found in soft tissues of the spine as well. These compounding effects introduce a large variation in the mechanical properties of cadaveric lumbar spines [39].

1.5.1 Cadaveric Models

In order to continuously create new products, make improvements on current products, and test techniques, doctors and engineers need reliable models to test and evaluate outcomes. An ideal model would have the following qualities:

- Anatomical and mechanical accuracy and precision
- Low inter-specimen variation
- Lengthy shelf life
- Repeatable test results
- Readily available to the consumer
- Relatively inexpensive

Currently, human cadavers represent the benchmark for all other models. Cadaveric models are unarguably anatomically and mechanically correct; they provide surgeons and engineers with opportunity to become familiar with hands on spinal anatomy, perform procedures with realistic variables, and analyze how the mechanics of a true spine are altered by implants or procedures. However, cadaveric models are not readily available. In order to obtain a specimen, researches must use organizations that collect specimens immediately post-mortem. Depending on the specifications of the specimen needed for the study, there may be (and normally are) long lead times,

sometimes a year, to find a viable specimen. At times, the desired specifications are not met; for example: if a L1 – L5 segment is requested, the specimen may arrive with half of L1 and a small portion of L5, which does not allow for adequate potting. In addition, cadaveric spines are often from older persons and also have high levels of osteoporosis, bone spurs, and other osteopaths that are not representative of the general population on which typical spine surgeries are performed. This issue is a concern of researchers as oftentimes surgeons are scheduled to perform procedures on these spines for testing, and if the specimen is not viable (incorrect segment, bone spurs, high degrees of osteoporosis), it is a waste of the surgeon's time and reflects poorly on the researchers or company. If a viable specimen can be found, the cost of obtaining such a specimen can high. In addition, specimens cannot be embalmed for preservation; they must be stored below -20°C to preserve their mechanical properties [40, 41]. It has also been shown that there is only a 20 hour window for testing of the thawed specimen. After the 20 hour window, the soft tissue of the specimen begins to degrade rapidly, and the stiffness of soft tissues decreases [42]. This drawback, in combination with viscoelastic properties of the spine, severally limits its ability to be used in fatigue testing. Furthermore, studies indicate that only three freeze-thaw cycles can be used before degradation of soft tissues of the spine occurs [43].

Inter-specimen variability is also a chief concern when using cadaveric models in studies. As people vary with size, strength, and metabolic health, so do cadaveric spines, which makes it difficult to find an "average" spine. Standard errors of mechanical stiffness of 100% or more can be anticipated between spines [44, 45]. Intradiscal pressure is another property that has been shown to have large variation (as much as five times) between spines [46]. These issues, amongst others, make it difficult for researchers to

ascertain what effects are due to the implant/procedure, test-setup, or variations in the specimen itself. It is especially difficult when generally small sample sizes are used due to the aforementioned difficulty of obtaining specimens.

1.5.2 Mechanically Accurate Models

Mechanically accurate models have been in use for some time. They have even been standardized by the American Society for Testing and Materials (ASTM). Standard ASTM F2077: Test Methods for Intervertebral Body Fusion devices gives the design layout of a commonly used model (Figure 6) [47].

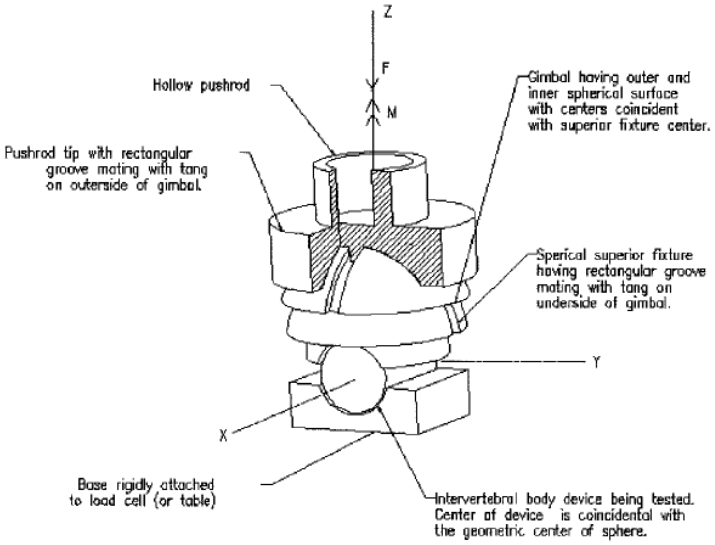

***Figure 6: A commonly used design layout for a mechanically accurate model recommended by ASTM standard F2077. Reprinted with permission from ASTM International* [47].**

These models are commonly used by researchers when cadaveric specimens are not a viable option. They are also oftentimes used for fatigue testing, since cadaveric specimens have such a short testing window. The models are typically assembled by the

labs using them and are composed of two rigid bodies that slide over one another or are connected by springs. While they are relatively easy to make and components that break or are damaged can easily be replaced, minimal, if any, attempt is made to make them anatomically correct. In addition, they don't accurately reflect the properties of cancellous bone or replicate the non-linear behavior of the spine. Another drawback is the challenge of fixation of implants that accompanies use in models that do accurately model cancellous bone. Screw toggling is a failure mechanism oftentimes seen in fatigue testing and if ignored, can cause serious drawbacks when the implant is tested *in-vivo*.

1.5.3 Anatomically Accurate Models

Anatomically accurate models are mainly used for show and educational purposes. They have varying degrees of anatomical accuracy but commonly show the vertebrae and intervertebral disc. Some models also include more soft tissues such as the musculature, innervation, and ligaments of the spine, which make them useful for initial training in a classroom environment. However, since there is no attempt to replicate the mechanical properties of the spine, they are not appropriate for use in testing of implants or procedures.

1.5.4 Numerical Models

Numerical models play an important role in early stage design of spinal implants. The level of sophistication, properties of hard and soft-tissue, and boundary conditions can all be controlled and customized by the researcher. In addition, computer models allow researchers to test on an "average" spine or alter the properties to evaluate the effects of

outliers and common pathologies. They can also simulate living tissue giving computer models the advantage to assess how the spine could react to certain aspects of implantation such as healing, bone remodeling in response to screw fixation, stress shielding, and adjacent level disc degeneration after spinal fusion.

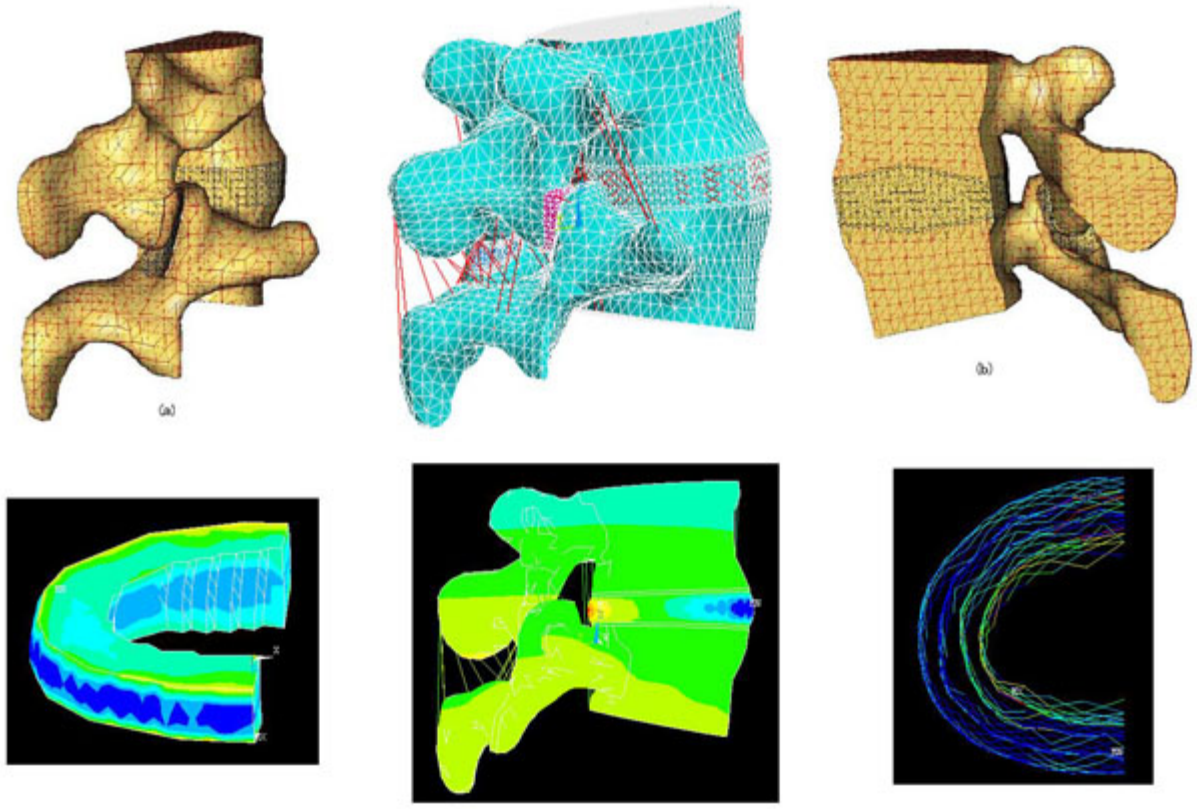

***Figure 7: Sample visual of computer models of portions of the spine. Reprinted with permission from Shanghai E-Feature Information Technology* [48].**

While numerical models are versatile, there are some drawbacks. These models are designed by the labs that use them and are not commercially available. This causes large variation in models and limits comparisons of studies from different labs. Also, only visual guidance (Figure 7) is allowed by computer models; hands-on experience (i.e.

implementation of a device by a surgeon's technique) cannot be obtained with the use of these models. The FDA also requires testing on physical models before approval can be obtained for marketing. Finally, the user must be well versed in the software package the model runs on and aware of the assumptions built in to the model which can limit its accuracy. Misunderstanding of the model details, assumptions, and appropriate applications can induce critical errors.

1.5.5 Analogue Spine Model

A solution is in development to address the previously described limitations. The Analogue Spine Model (ASM) has been developed to accurately model both the anatomical and mechanical properties of the human lumbar spine (Figure 8) [49, 50].

Figure 8: One version of the Analogue Spine Model.

Previous work has been completed to model each element of the spine, both mechanically and anatomically, and assembled in such a way that the model behaves like an "average" cadaveric spine [51]. The development of the ASM has been an ongoing joint effort between the University of Kansas and Pacific Research Laboratories (PRL) funded in part by grants from the National Institute of Health (NIH).

The composite material used to simulate the cortical bone of the model has undergone substantial development. After approximately 20 years, it is now in its fourth generation. The cortical bone is modeled by a short fiber epoxy composite, which has undergone significant testing of stress/strain behavior, crack propagation, and fatigue testing to ensure its accuracy when compared with its human counterpart. In addition, an effort was made to accurately model the vertebral geometry at each level of the lumbar region.

The cancellous bone used in current Sawbones® (PRL) models is closed-cell foam. In order to accurately model human cancellous bone, open-celled foam needed to be developed. Current open-celled foams on the market do not accurately model the mechanical properties of human cancellous bone [52]. Researchers from the two sites collaborated to develop the manufacturing techniques needed to produce an open-cell foam that would have the desired properties [53]. Several resins were evaluated using foam theory for their potential effectiveness for use in the production of the required foam. Once the required research was accomplished, further work was completed to incorporate the cortical shell.

Spinal ligaments have been developed and characterized to ensure they have appropriate dimensions and mechanical properties as reported in literature [50, 54]. Most

of the effort was placed on the design of the anterior longitudinal ligament (ALL) and the posterior longitudinal ligament (PLL). It was demonstrated that changes in the properties of these ligaments can effectively control the mechanical performance of the ASM.

Lost-wax molds of human intervertebral discs (IVDs) were made of each level of the lumbar spine to ensure the synthetic equivalent would be customized to the specific level of the spine. The initial attempts at creating the synthetic IVDs used polyester fibers embedded in a polyurethane matrix in order to recreate the 30° fibrous morphology. These attempts were unsuccessful, as manufacturing obstacles were encountered and other performance related issues could not be solved (such as failure along fiber boundaries). A simplified design was adopted; currently a single woven sheet of polyester fibers is attached to the vertebrae and wrapped around the entire disc containing the disc. The approach increases durability while still imparting non-linear behavior into the model. A gel-like isotropic polyurethane of low durometer was chosen for the nucleus pulposus for its ability to evenly transfer hydrostatic pressure to the adjacent endplates. After construction of the IVDs, compression testing was completed to ensure that the synthetic disc performed similar to human IVDs as reported in the literature [55-56].

The facet joints also received substantial consideration. After several attempts, a "reverse synovial joint" was utilized. Each end of the opposing facets was covered with wax, and then covered with a low durometer polyurethane. When these joints are compressed the wax shears out of the way, acting as synovial fluid, and the polyurethane coating acts as the articular cartilage. The manufacturing process was also considered and altered to allow for rapid, repeatable construction.

Currently the model does not include a bone marrow component. While not mechanically relevant, bone marrow does have an effect on bone cement intrusion. Techniques such as brushing (removing surface debris) and pressurized lavage (removing marrow from bone interstices) used in preparation for the bone-cement interface during surgical procedures has been shown to improve cement intrusion into the cancellous bone. The use of a pressurized lavage increased cement intrusion from 0.2 mm to 4.8 mm resulting in increased shear strength from 1.9 MPa to 26.5 MPa over untreated bone surfaces, proving marrow's effect on cement intrusion [57]. Not much research has been completed on marrow's effects on bone cement augmentation of pedicle screws; however, the aforementioned indicates that marrow may play a key role in the contribution to bone cement intrusion and performance of anchoring bone screws.

The objective of this study is to:

1) Identify an appropriate material with similar qualities as human bone marrow that is readily available and inexpensive
2) Assess the effects of the synthetic marrow on the material properties of the resins used to produce the synthetic cortical and cancellous bone, and,
3) Assess the long term (shelf-life) effects of the material on the cancellous foam and evaluate any changes in mechanical properties

Chapter 2: Effect of Synthetic Marrow on Resin of Synthetic Trabecular Bone

2.1 Introduction

A first generation of the ASM has been developed by PRL, to anatomically and mechanically replicate the human lumbar spine. A synthetic bone marrow is being introduced to improve this model for use in some types of mock surgical procedures. Currently the ASM does not include a bone marrow component. While not mechanically relevant, bone marrow does have an effect on bone cement intrusion. Techniques such as brushing (removing surface debris) and pressurized lavage (removing marrow from bone interstices) used in preparation for the bone-cement interface during surgical procedures have been shown to improve cement intrusion into the cancellous bone. The use of a pressurized lavage increased cement intrusion from 0.2 mm to 4.8 mm resulting in increased shear strength from 1.9 MPa to 26.5 MPa over untreated bone surfaces, proving the effect of the marrow on cement intrusion [57]. In addition, bleeding in bone during cement intrusion can decrease shear strength of the bone-cement interface as much as 50% [58]. The aforementioned indicates that marrow may play a key role in bone cements' contribution to anchoring bone screws.

Preliminary work identified glycerin as a candidate for use as a yellow marrow substitute due to its viscosity and availability. To ensure the viability of the synthetic bone marrow, a study must be performed to test the effects of the marrow on the materials used to produce the current analogue cortical and cancellous bone. The synthetic marrow must not alter the mechanical properties of these materials after prolonged exposure; as this would significantly reduce the shelf life of the proposed product. The purpose of the

present study is to determine the effect of exposure of the synthetic marrow, glycerin, on the resins used to create the synthetic cortical and trabecular bone. In this work, two resins used to make cortical and cancellous bone for the ASM are exposed to the proposed synthetic bone marrow. Material properties were measured over a period of timed exposure to the marrow.

2.2 Materials and Methods

A total of 36 analogue bone material specimens were used for this study, split between two proprietary materials A & B, that are resins used in the development of synthetic cortical and trabecular bone, respectively [53]. The materials were mixed in the same environment used in ASM bone manufacturing and poured into sheets of 2.0 mm thickness. Specimens were then cut to their final dimensions (50.0 x 12.5 x 2.0 mm) by a CNC machine. Each specimen was measured at three locations along each of the three dimensions prior to testing. At least six specimens (n=6) were tested for each of the following conditions:

- Dry, no soaking (control)
- Two week soak in glycerin solution
- Four week soak in glycerin solution

Specimens were tested in accordance with ASTM D6272 – 10 "Standard Test Method for Flexural Properties of Unreinforced and Reinforced Plastics and Electrical Insulating Materials by Four-Point Bending" [59]. The specimens were tested using a MTS 858 Mini Bionix Hydraulic Materials Testing Machine (Eden Prairie, MN) equipped with a

25 kN load cell (±X.XX N; sampling rate of 100 Hz) to measure the axial force on the specimen. Displacement was measured of the upper platen relative to the lower platen with the built in LVDT (±0.01 mm; sampling rate of 100 Hz). While this was not a true midpoint displacement measure, as specified by the ASTM standard, it is acceptable for this study as specific material properties were not of interest, only the relative change in material properties due to the material's exposure to glycerin was of concern. The jig had cylindrical loading noses per the ASTM Standard with the loading span (12.59 mm) equal to one half the distance of the support span (25.85 mm) with radii of 5.13 mm. All measurements were taken after jig assembly with digital calipers (± 0.01 mm).

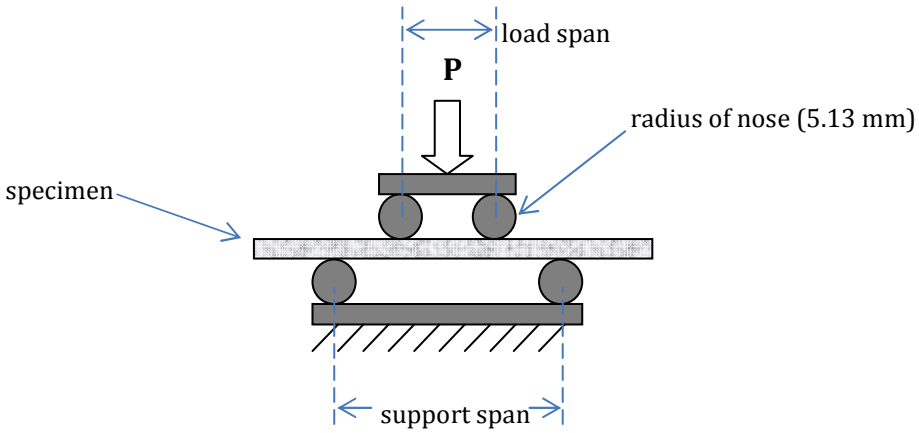

Figure 9: Four-point bend test setup. The light grey rectangle is the test specimen; the dark grey shapes are the jigs used for testing. Force (P) was applied to the top jig; the bottom jig was immovable and fixed to the load detector (not shown).

The specimens were placed on lower supporting noses of the four point bend jig and visually centered (Figure 10). The upper loading noses were lowered to a starting position

slightly above the specimen. For testing, a strain rate of 5.07 mm/min was used which was determined by Equation 1, as given in ASTM D6272. Specimens were tested until a strain of 5 percent was achieved or specimen fracture occurred.

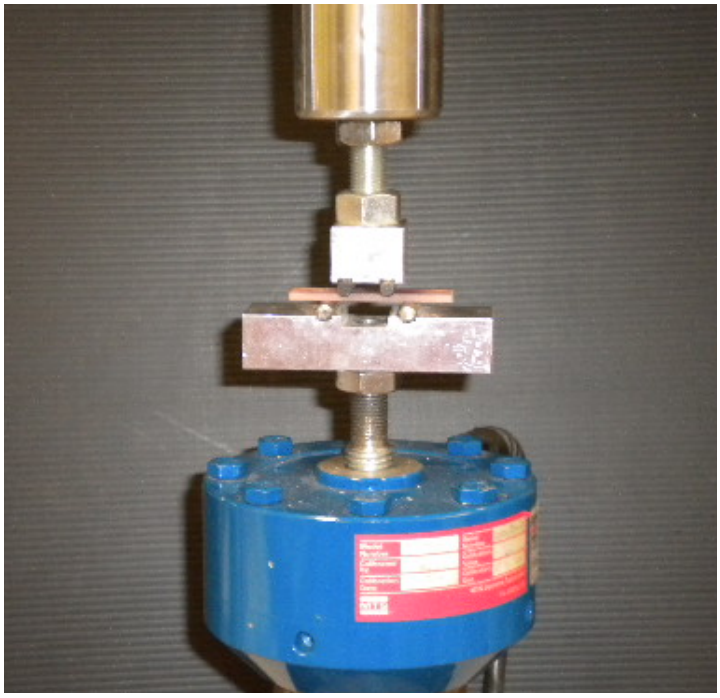

Figure 10: Picture of the test set-up for the four point bending tests.

$$R = \frac{0.167 \cdot Z \cdot L^2}{d} \left(\frac{mm}{min}\right)$$

Equation 1: Strain rate in a four-point bend specimen.

Maximum stress, maximum strain, and modulus of elasticity were calculated using Equations 2, 3, and 4 provided by ASTM D6272. Maximum displacement of the loading platens relative to one another was used as the maximum deflection of the center of the

four-point bend specimen (D) in Equation 3, thus the true maximum strain was not calculated.

$$\sigma = \frac{3 \cdot P \cdot L}{4 \cdot b \cdot d^2} \ (MPa)$$

Equation 2: Maximum stress in a four-point bend specimen.

$$\varepsilon = \frac{4.36 \cdot D \cdot d}{L^2} \ \left(\frac{mm}{mm}\right)$$

Equation 3: Maximum strain in a four-point bend specimen

$$E = \frac{0.17 \cdot L^3 \cdot m}{b \cdot d^3} \ (MPa)$$

Equation 4: Modulus of elasticity in a four-point bend specimen.

R – rate of crosshead motion (mm/min)

Z – rate of straining of the outer fibers (shall equal 0.01 mm/mm per ASTM Standard)

L – support span (mm)

d – depth of beam (mm)

σ – maximum stress of specimen (MPa)

P – load at a given point on the load-deflection curve (N)

b – width of beam (mm)

ε – maximum stress of specimen (mm/mm)

D – maximum deflection of center of beam (mm)

E – modulus of elasticity in bending (MPa)

m – slope of tangent to the initial straight-line

2.3 Results

2.3.1 Material "A" Results

The average modulus of the control group of material A (analogue cancellous bone resin) was 5.36 GPa with a coefficient of variation (COV = standard deviation / average) of 1.4%. The 2 week soaked group showed a similar amount of variation (1.3%) with an average modulus of 5.35 GPa. The 4 week soaked group proved to have a lower average modulus (5.06 GPa) and more variation (2.3%). A one-way ANOVA was performed and a statistically significant difference was found between the three groups. However, when a t-test was performed ($\alpha = 0.05$) between the control group and the 2 week soaked group, no statistically significant difference was found between the two groups. There was a significant difference between the control and 4 week groups and between the 2 week and 4 week groups (Figure 11; Table 6). The material A samples performed as would a highly elastic, stiff rubber; consequently, yield stress, yield strain, ultimate stress, and ultimate strain were not reported, as the test jigs used did not allow the material A specimens to be deformed to the extent that would produce yielding.

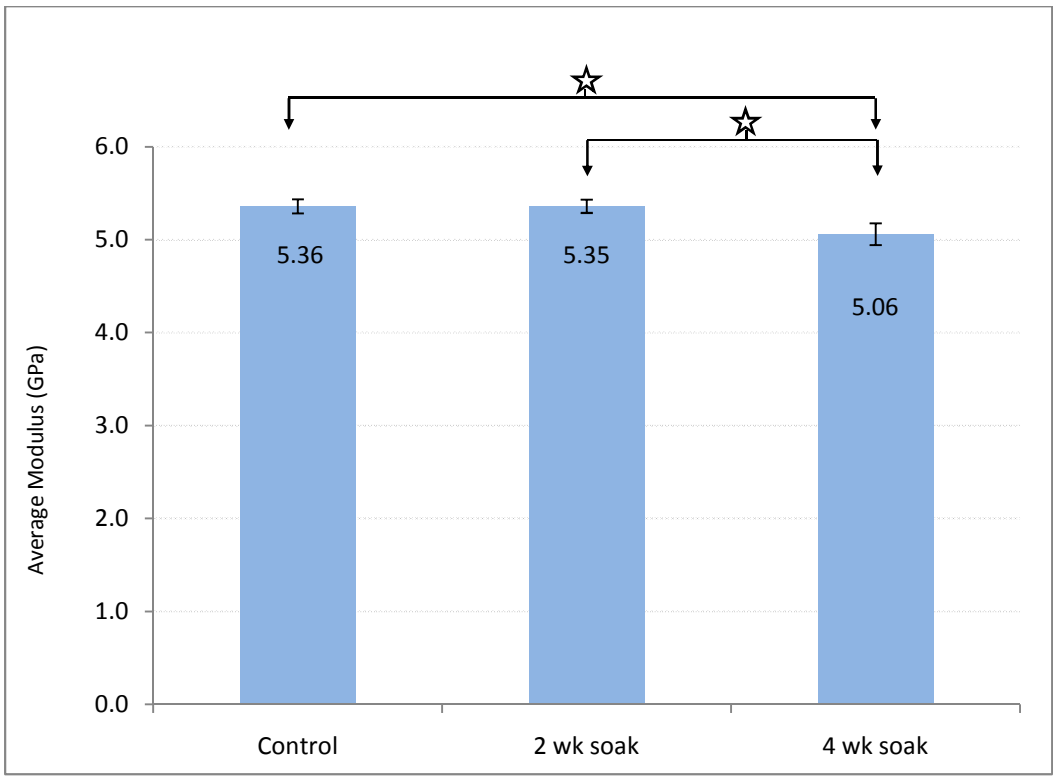

Figure 11: Material "A" (resin for analogue cancellous bone) average modulus (stars indicate significance in t-test, p-values at $p \leq 0.05$).

Table 6: Results and statistics for moduli calculations in Material A ($n = 6$; $\alpha = 0.05$).

Material "A" Average Modulus			
	Control	**2 wk soak**	**4 wk soak**
Average (GPa)	5.36	5.35	5.06
Std Deviation	0.075	0.071	0.118
COV	1.4%	1.3%	2.3%
p-value from ANOVA	***0.00004***		
t-test (control & 2 week)	0.862		
t-test (control & 4 week)	***0.001***		
t-test (2 week & 4 week)	***0.001***		

2.3.2 Material "B" Results

The material B (analogue cortical bone resin) samples were brittle, thus the yield and ultimate stress and strains were found to indistinguishable, and therefore, the yield stress and strains are unreported to alleviate redundancy.

The average modulus of the control group was 24.3 GPa with a COV of 5.3%. Similarly, the modulus of the 2 week soaked group was 25.3 GPa with a COV of 5.2%. The 4 week soaked group showed a much lower modulus than the other groups, reporting a value of 21.1 GPa, and a higher amount of variation (COV = 15.4%). The three groups were found to have a statistically significant difference by one-way ANOVA ($p = 0.0131$, $\alpha = 0.05$). When comparing the control group to the 2 week and 4 week soaked groups, no significant difference was found by t-test ($p = 0.238$, $p = 0.067$, respectively; $\alpha = 0.05$). Only the 2 week and 4 week soaked group showed significance by t-test ($p = 0.027$; Figure 12; Table 7).

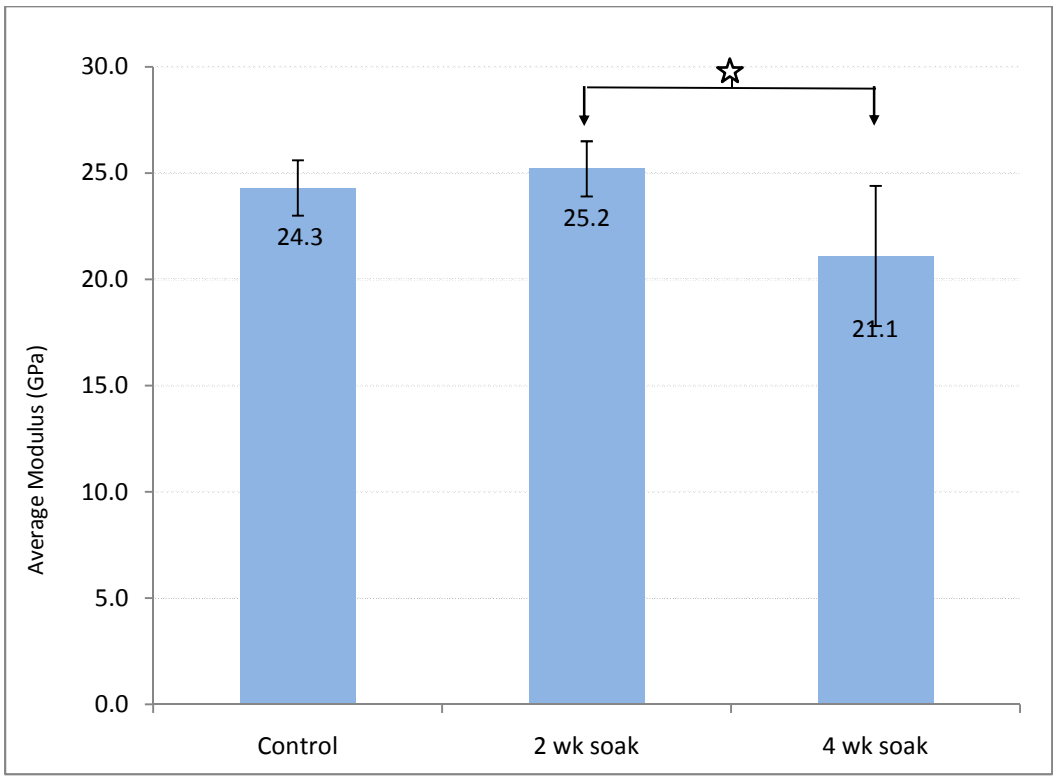

Figure 12: Material "B" (resin for analogue cortical bone) average modulus (star indicates significance in p-value of t-test, p-values at $p \leq 0.05$).

Table 7 : Results and statistics for moduli calculations in Material B ($n = 6$; $\alpha = 0.05$).

Material "B" Average Modulus			
	Control	**2 wk soak**	**4 wk soak**
Average (GPa)	24.3	25.2	21.1
Std Deviation	1.29	1.31	3.26
COV	5.3%	5.2%	15.4%
p-value from ANOVA	***0.013***		
t-test (control & 2 week)	0.238		
t-test (control & 4 week)	0.067		
t-test (2 week & 4 week)	***0.027***		

Similar to the modulus, the average ultimate stress of the control group and the two week soaked group were similar (233 and 236 MPa, respectively). The average ultimate stress of the 4 week soaked group was higher, with a value of 244 MPa; however, no statistically significant difference was found between the three sample groups by one-way ANOVA ($p = 0.592$; $\alpha = 0.05$) or by t-test of the paired groups (Table 8). The highest COV was found in the control group (9.4%), and the lowest COV was found in the 2 week soaked group (5.8%).

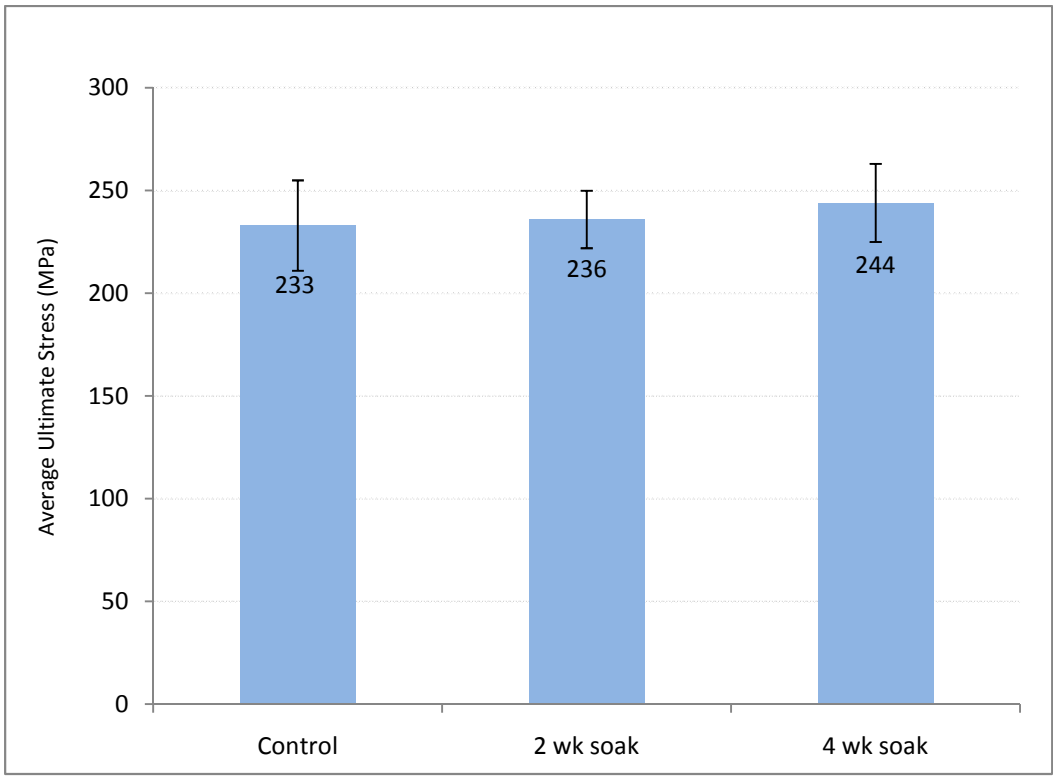

Figure 13: Material "B" average ultimate stress.

Table 8: Results and statistics for ultimate stress calculations in Material B (n = 6; α = 0.05).

Material "B" Average Ultimate Stress			
	Control	**2 wk soak**	**4 wk soak**
Average (MPa)	233	236	244
Std Deviation	22	14	19
COV	9.4%	5.8%	7.9%
p-value from ANOVA	0.592		
t-test (control & 2 week)	0.824		
t-test (control & 4 week)	0.391		
t-test (2 week & 4 week)	0.415		

The control group and the 2 week soaked group had similar values for average ultimate strain, 0.011 and 0.011 mm/mm, respectively. The average ultimate strain in the 4 week soaked group was markedly higher with a value of 0.013 mm/mm. The COVs were all below 10%. ANOVA analysis showed statistically significant difference between the three groups (Table 9). T-test analysis showed significance between the control group and 4 week soaked group and between the 2 and 4 week soaked groups (Figure 14).

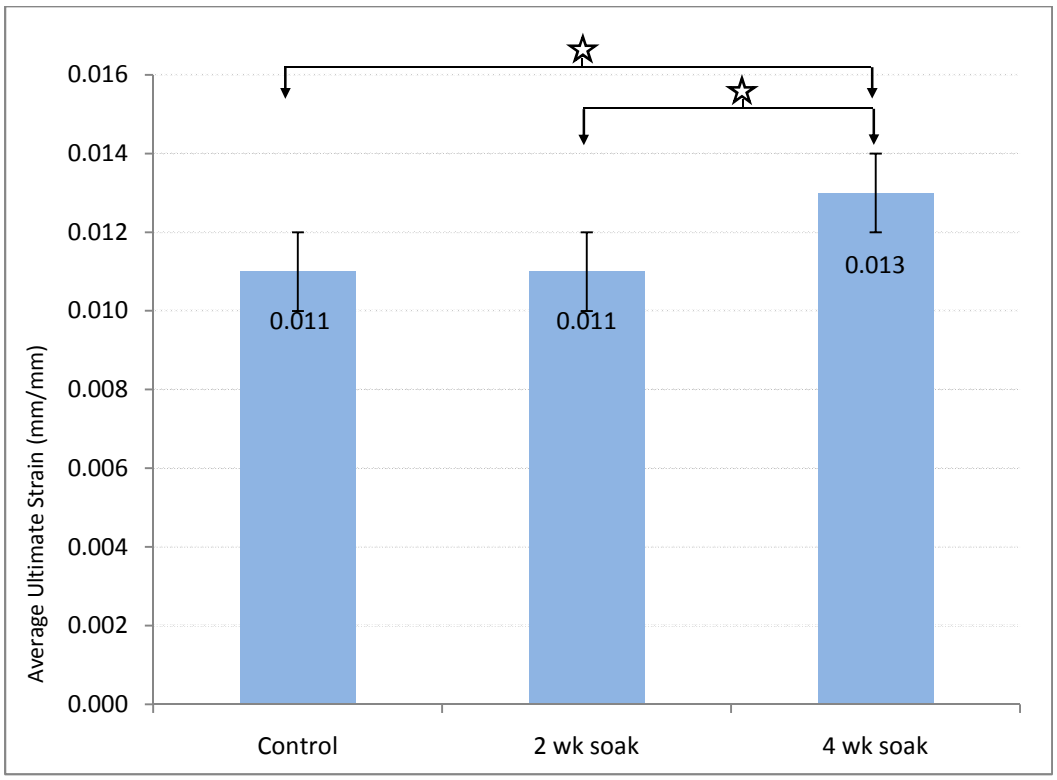

Figure 14: Material "B" average ultimate strain (stars indicate significant p-values from t-test, p-values at p ≤ 0.05).

Table 9: Average ultimate strain of material B and statistical analysis (n = 6; α = 0.05).

Material "B" Average Ultimate Strain			
	Control	**2 wk soak**	**4 wk soak**
Average	0.0111	0.0107	0.0127
Std Deviation	0.0008	0.0005	0.0012
COV	7.2%	4.7%	9.4%
p-value from ANOVA	***0.013***		
t-test (control & 2 week)	0.346		
t-test (control & 4 week)	***0.022***		
t-test (2 week & 4 week)	***0.007***		

2.4 Discussion

As previously stated, materials A and B are proprietary resins used in the manufacturing process of cancellous and cortical bone, respectively [53]. These resins control the mechanical properties of the end product, thus are the focus of this study. Material A is more ductile, and has been found to properly replicate cancellous bone when used in the patented manufacturing process [53]. Material B is less ductile and stronger, therefore better suited to model the denser cortical bone.

2.4.1 Material "A" Discussion

One-way ANOVA analysis revealed that the average modulus of the three groups (control, 2 week soak, 4 week soak) were significantly different. In comparing the groups by individual t-test, the average moduli of the control and the 2 week soaked samples were not found to be statistically different. However, the 4 week soaked samples showed statistically significant differences when compared with the control and 2 week soaked samples independently. This shows that the material's properties may have begun to alter after the initial two weeks of soaking.

Table 10 compares the results of the current study to values for individual trabeculae and micro scale specimens of cancellous bone found in literature. As previously mentioned, the values reported for properties in this study are not exact, as center point deflection was not measured; rather displacement of the loading noses was recorded. Figure 15 shows the displacement measured (x), and the correct measurement called for by the ASTM standard (x'). This can cause an underestimation of the modulus as the slope of the tangent to the initial straight line on the load-deflection curve would decreased due

to the lower estimation of the deflection. Figure 16 shows the resultant effect of the alternative measurement on the load-deflection curve. No attempt to correct this was made, as it would introduce a new assumption which cannot be shown to be accurate with the limitations presented in product development. In addition, measurement techniques and calculations were consistent between materials and groups. With this in mind, comparing the values of the current study to values from literature can give a better understanding of the material presented. The values for modulus from the study fall within the range of values reported. The standard deviation of the study in all groups was significantly lower than the majority of reports from the literature. This is important as a major goal of the ASM is consistency and precision of its mechanical properties.

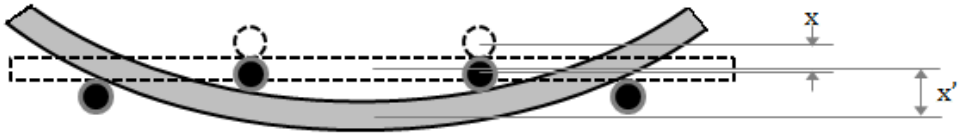

Figure 15: Exaggerated image of four-point bending. The correct measurement for mid-point deflection (x'), and the recorded deflection (x) in the four point bending tests. In this case, x' > x.

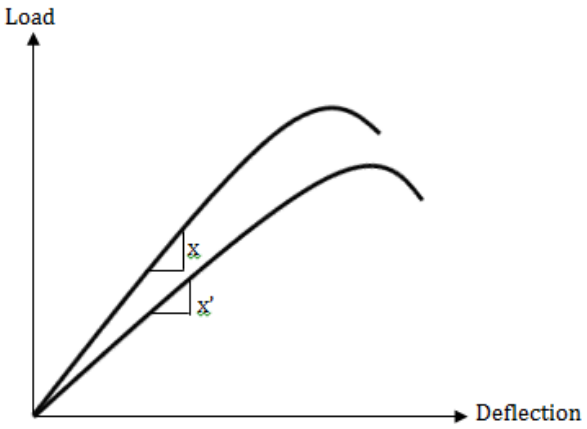

Figure 16: The resultant effect on the load deflection curve from the measurement of deflection recorded; "x'" is the true load-deflection and, "x" is the recorded load-deflection curve. The slope of the tangent to the initial straight line of the curve is decreased (x' > x).

***Table 10: Current study and literature values for the modulus of resins and cancellous bone. Table adapted from Rho et al.* [60].**
[1]micro-scale specimens
[2]individual trabeculae

Author	Year	Test Method	Avg Modulus (GPa)	Std Dev (GPa)
Current Study (control)	2011	4-pt bending	5.36	0.075
Current Study (2 wk soak)	2011	4-pt bending	5.35	0.071
Current Study (4 wk soak)	2011	4-pt bending	5.06	0.118
Choi / Goldstein [61]	1992	4-pt bending[1]	5.72	1.27
Kuhn et al. [62]	1989	3-pt bending[2]	3.81	---
Ryan / Williams [63]	1989	tensile (bovine)[2]	0.760	0.390
Choi et al. [64]	1990	3-pt bending[1]	4.96	1.85
Rho et al. [65]	1993	tensile[2]	10.4	3.50

2.4.2 Material "B" Discussion

Material B (i.e., the resin used in producing analogue cortical bone) showed significant difference between the three groups, which can be traced to the 4 week soaked samples as shown by t-test analysis. This may have been a result of increased penetration of the synthetic marrow in the samples causing the samples to plasticize. The only property to not exhibit any significant difference by any measure was ultimate stress of material B.

Table 11 compares the results of the current study to values of stiffness for cortical bone in literature. The values from this study are higher than those reported in the literature; however, the specimens used in the study were solid whereas cortical bone does include a degree of porosity and variable quality, thus direct comparison to literature values should be made on a magnitude scale only. In addition, Choi and Goldstein used micro-scale specimens that did not meet ASTM specifications which could limit the accuracy, thus the nanoindentation studies by Turner et al. are a better indication of the true modulus of cortical bone [61, 66]. The standard deviations found in the current study materials are lower than the majority of the literature data reported. This shows that the cortical bone resin is more precise and reliable than its human counterpart.

Table 11: Current study and literature values for the modulus of resins and cortical bone.

Author	Year	Test Method	Avg Modulus (MPa)	Std Dev (MPa)	Orientation
Current Study (control)	2011	4-pt bending	24.3	1.29	n/a
Current Study (2 wk soak)	2011	4-pt bending	25.2	1.31	n/a
Current Study (4 wk soak)	2011	4-pt bending	21.1	3.26	n/a
Choi / Goldstein [61] (milled)	1992	4-pt bending	6.75	1.00	longitudinal
Choi / Goldstein [61] (unmilled)	1992	4-pt bending	6.48	1.61	longitudinal
Yang / Lakes [67]	1982	coupling	14.4	3.26	longitudinal
Turner et al. [66]	1999	nanoindentation	16.58	0.32	transverse
Turner et al. [66]	1999	nanoindentation	23.45	0.21	longitudinal

There were many limitations to the study, which include:

1. There was limited control over the specimens in this study. The specimens were manufactured at PRL, thus, the age of the specimens was unknown.
2. The specimens were manufactured and stored in an unknown environment at PRL.

3. Limited information was given about the manufacturing protocol itself was known. If the specimens were manufactured in different batches or stored for different periods the data may be inaccurate. While this is a limitation in the study, it does represent the true production process of the end product.
4. In addition, after further review, age changes in the samples were not measured; however, the specimens were allowed to age approximately six months at room temperature prior to testing, thus the testing length (4 weeks) was minimal in comparison.

2.5 Conclusion

Material A has shown that its material properties may change after prolonged exposure to the synthetic marrow, and material B displayed some indication that its material properties were affected by the synthetic marrow. The data does not show a substantial or conclusive degradation of properties, but with the shelf life of the Analogue Spine Model anticipated to be longer than the durations in this study, it is necessary to run further tests. Since material A did not yield, other modes of testing, such as tensile tests, should be considered. In addition, it should be noted that only the resins were tested, not the end product. Further tests should include samples of the open-celled foam tested in modes that are relevant to the ASM such as compression and bone screw pullout.

Chapter 3: Effect of Synthetic Marrow on Synthetic Trabecular Bone by Compression and Bone Screw Pullout

3.1 Introduction

A first generation of the Analogue Spine Model has been developed by Pacific Research Laboratories, to anatomically and mechanically replicate the human lumbar spine. To improve this model a synthetic bone marrow is being introduced. Currently the model does not include a bone marrow component. While not mechanically relevant, bone marrow does have an effect on bone cement intrusion. Techniques such as brushing (removing surface debris) and pressurized lavage (removing marrow from bone interstices) used in preparation for the bone-cement interface during surgical procedures has been shown to improve cement intrusion into the cancellous bone. The use of a pressurized lavage increased cement intrusion from 0.2 mm to 4.8 mm resulting in increased shear strength from 1.9 MPa to 26.5 MPa over untreated bone surfaces, proving marrow's effect on cement intrusion [57]. Not much research has been completed on marrow's effects on bone cement augmentation of pedicle screws; however, the aforementioned indicates that marrow may play a key role in the contribution to bone cement intrusion and performance of anchoring bone screws.

To ensure the viability of the synthetic bone marrow, two key tasks must be addressed. First, a material must be selected that has similar qualities as human bone marrow, and second, a material that does not degrade or alter the mechanical properties of the existing synthetic trabecular bone in the model. A material has already been selected that has shown to have a similar viscosity to bone marrow [53]. The purpose of this study

is to determine the effects of prolonged exposure of the analogue cancellous bone to the synthetic bone marrow.

This work is necessary to increase the validity of the model for research applications such as bone cement intrusion, vertebroplasty, and kyphoplasty studies, and to a much lesser extent model the hydrostatic pressure within the vertebral body.

3.2 Materials and Methods

The material used in this study was a rigid polyurethane open-cell foam with a proprietary blend of polyurethane, glass, and lime manufactured using a technique developed and patented by Pacific Research Laboratories (PRL) [53]. A total of 6 rectangular test blocks (130 x 180 x 40 mm) were produced in three separate batches (2 blocks per batch) on different days. This was done to not only asses the foam properties, but also inter-batch variability. The batches were denoted A, B, and C, and the test blocks were denoted 1 and 2; thus giving blocks of A1, A2, B1, B2, C1, and C2 (Figure 17). Each of the test blocks were cut with a MicroLux Mini Tilt Arbor Table Saw with diamond blade from Micro Mark (Berkley Heights, NJ) to provide 12 compression specimens (20 x 20 x 40 mm) and 6 pullout specimens (25.4 x 25.4 x 50.8 mm) to be used for the bone screw pullout tests. The hierarchy of the samples can be seen in Figure 17. The location the specimens were taken from can be seen in Figure 18.

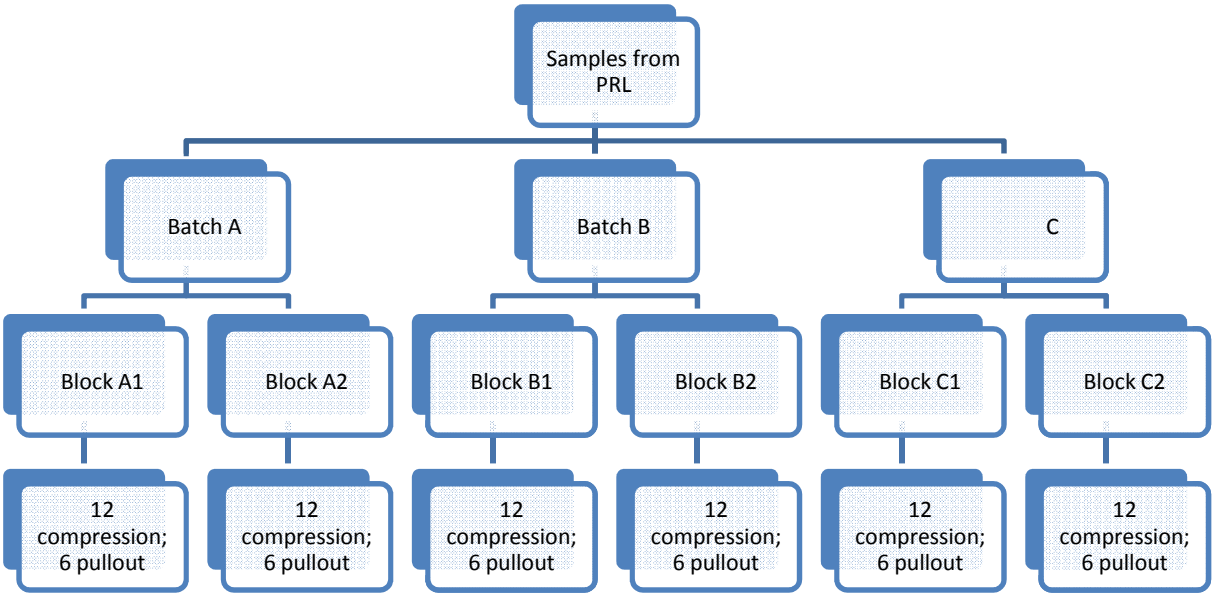

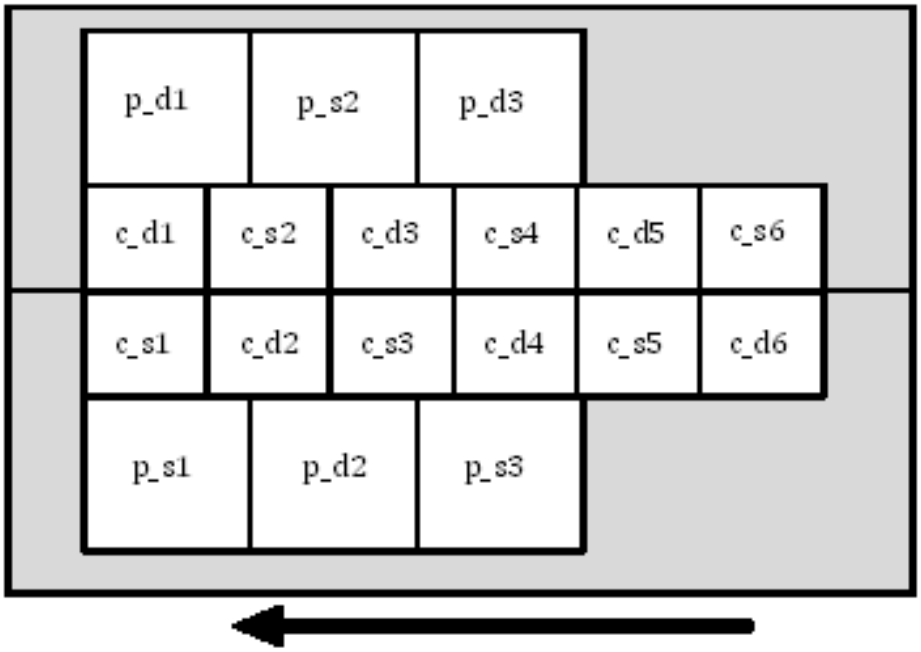

Figure 18: Locations of the test specimens. The black arrow indicates direction of processing. The grey portion of the test block was unused.

Individual specimens were denoted as X_YZ, where:

- X: pullout or compression specimen (c or p)
- Y: dry specimen or soaked specimen (d or s)
- Z: specimen number (1-3 for bone screw pullout, 1-6 for compression)

The leading edge (10 mm) of the test block was trimmed so that the edge effects produced during the manufacturing process would not affect the outcome of the testing of the compression specimens. Each specimen was individually inspected for abnormalities and atypical voids (larger than 10 mm).

All specimens were measured in three different locations for each of the three dimensions (length, width, height) to the nearest 0.01 mm using digital calipers. An average of each of these measurements was found and the total volume calculated. The mass of each specimen was measured to the nearest 0.01 g. From these measurements, the density of each specimen was calculated.

Thirty –six compression specimens and eighteen bone screw pullout specimens (six compression and three bone screw pullout specimens from each test block) were soaked in a synthetic bone marrow component solution consisting of glycerin (www.ScienceCompany.com, 99.5% purity) and purified water (44.5% glycerin by weight). The container used for soaking was kept airtight so as to keep the glycerin solution from absorbing water from the environment. The specimens were soaked for a duration of 4 weeks, on which day they were tested. The specimens remained in the solution and were removed one at a time when test preparation commenced. During test preparation, the specimens were wrapped with a cloth soaked in the glycerin solution to reduce the amount

of drying during preparation. On completion of the testing preparation, the wrap was removed and testing was immediately initiated. All dry, unsoaked specimens were tested in their native, untreated forms.

3.2.1 Compression Testing

Compression specimens were tested in close accordance with ASTM D1621 – 10 "Standard Test Method for Compressive Properties of Rigid Cellular Plastics" when appropriate [68]. Twelve specimens from each test block were tested in compression (6 dry, untreated specimens; 6 glycerin soaked specimens). A significant source of variation arises if the ends of the specimens are placed in direct contact with the loading platens. This occurs due to frictional forces acting on individual free struts (end artifacts) of the foam, and in previous research, this has been shown to cause an overestimate the modulus and yield strain of human trabecular bone by 40% [33]. To remedy this effect, the compression specimens were potted in 3.70 mm of Bondo in a custom designed mold to ensure the ends were perpendicular to the length of the specimen. Each specimen was potted at least 24 hours prior to testing to allow adequate time for the Bondo to fully cure and achieve its maximum mechanical properties. The glycerin soaked specimens were also potted in this fashion; however they were wrapped in a cloth soaked in the glycerin solution during the potting and curing process in order to reduce drying.

The testing was carried out with using a MTS 858 Mini Bionix Hydraulic Materials Testing Machine (Eden Prairie, MN). After the potting and curing process, the specimens were placed on the lower, self-aligning platen of the test machine and visually aligned so

that the center-line of the specimen was in line with the center-line of the loading axis of the test machine (Figure 19).

Figure 19: Test set-up for compression tests.

The testing machine was equipped with a 2.5 kN load cell to measure the axial force on the specimen. Initially, the specimens were subjected to a 5 N preload. They were then cycled five times to a 0.5% strain (=0.2 mm) with a sine wave profile at 1 Hz (preconditioning). The compressive load was then returned to 5 N. The specimens were then loaded to failure at a rate of 0.05 mm/sec. Data was recorded (load and platen displacement) at a rate of 100 Hz during the final compression.

3.2.2 Bone Screw Pullout Testing

Bone screw pullout specimens were tested in with close accordance with ASTM F 1839 – 01 (2007) "Standard Specification for Rigid Polyurethane Foam for Use as a Standard Material for Testing Orthopedic Devices and Instruments" [69]. Pilot holes (3.2 mm) were drilled in each specimen and all particulate debris was removed. The pilot holes were not tapped as specified by the ASTM standard, as a self-tapping screw was used to limit the amount of variation introduced to the study. A bone screw (outside diameter (od) 6.2 mm; inner diameter (id) = 4.0 mm, threads per inch (TPI) = 9.2) (Figure 20) was inserted through a bushing into the specimen by a drill press at a rate of approximately 6.0 rev/min to a depth of 20 mm (Figure 21). The bushing also served as a custom designed pulling jig (Figure 22). The pulling jig was cylindrical in shape and had a through-hole 1 mm wider than the major diameter of the screw head. A second hole was cut into the jig that was larger than the screw head with a spherical recess in which the screw head rested. This spherical recess acted as a universal joint.

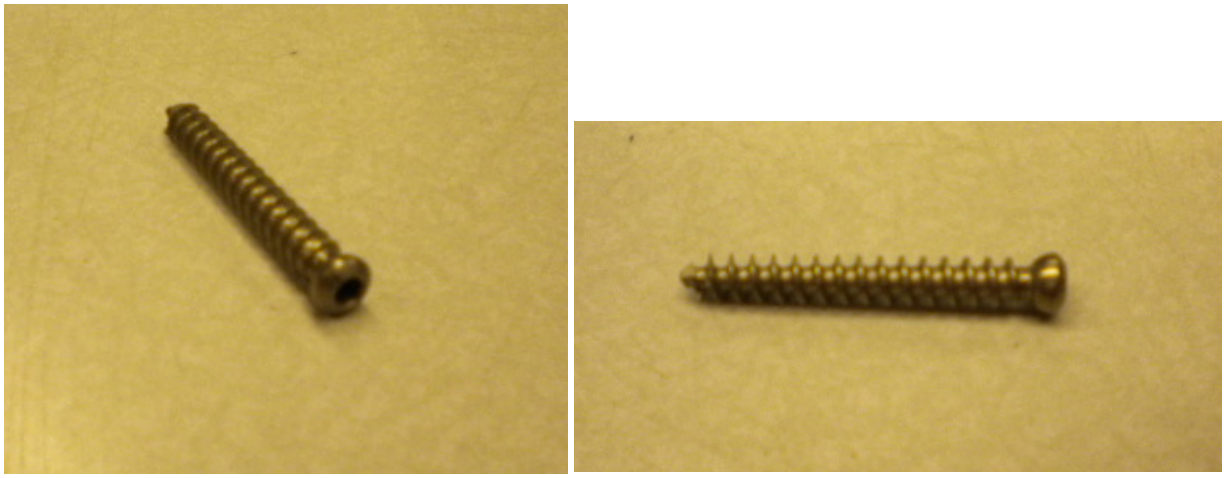

Figure 20: Bone screw used in the pullout study.

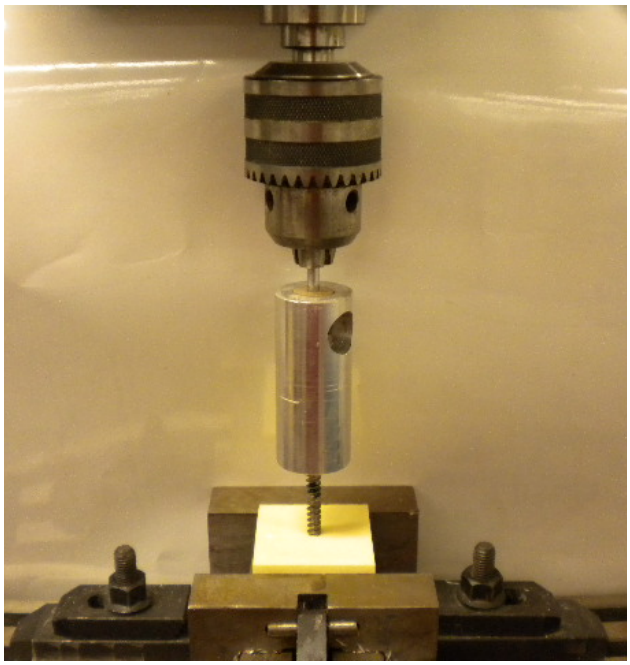

Figure 21: Bone screw insertion set-up.

The test specimen with the screw inserted through the pulling jig/bushing was then attached to the MTS 858 Mini Bionix Hydraulic Materials Testing Machine (Eden Prairie, MN) and visually aligned so that the pulling axis was in line with the screw to insure only axial forces acted on the screw. The test specimen was then secured to the test block clamp fixed to the lower portion of the test machine in a manner to protect the integrity of the alignment of the loading axis (Figure 22). The screw was then loaded to failure at a rate of 5 mm/min. The ultimate failure load was defined as the maximum force required to remove the screw from the test block. All specimens from all test blocks were tested in this manner. The soaked specimens remained in the solution until the screw was to be inserted and testing completed.

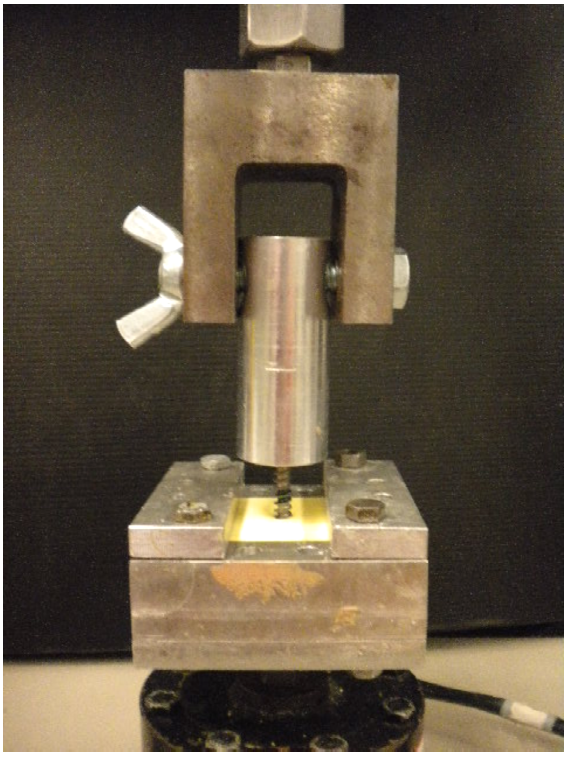

ure 22: Bone screw pullout test set-up.

3.3 Results

The following results were calculated using Matlab (MathWorks; Natick, MA) and statistical evaluation was completed using Microsoft Excel (Microsoft; Redmond, WA).

3.3.1 Compression

No statistically significant differences in modulus, yield stress, yield strain, ultimate stress, or ultimate strain were found when comparing dry compression specimens from blocks within the same batch by t-test. When grouping the dry samples by batch to check for interbatch variability by one-way ANOVA, no significance was seen in all of the aforementioned properties except yield strain which produced a value of 0.006, showing a significant difference between batches. Tables 12 and 13 shows the results of the dry specimens with groupings by block and batch, respectively.

Table 12: Compression test results by block (dry specimens only).

	Moduli (MPa)					
Block	**A1**	**A2**	**B1**	**B2**	**C1**	**C2**
Average	356	383	417	359	374	327
Standard Deviation	31.8	47.8	58.0	25.6	115.6	53.9
t-test (p-value)	0.374		0.103		0.494	
	Yield Stress (MPa)					
Block	**A1**	**A2**	**B1**	**B2**	**C1**	**C2**
Average	3.45	4.21	3.89	3.59	4.19	3.52
Standard Deviation	0.41	0.72	0.58	0.72	0.76	0.45
t-test (p-value)	0.123		0.578		0.171	
	Yield Strain (mm/mm)					
Block	**A1**	**A2**	**B1**	**B2**	**C1**	**C2**
Average	0.0133	0.0158	0.0133	0.0135	0.0168	0.0156
Standard Deviation	0.0021	0.0033	0.0024	0.0033	0.0046	0.0028
t-test (p-value)	0.237		0.926		0.493	
	Ultimate Stress (MPa)					
Block	**A1**	**A2**	**B1**	**B2**	**C1**	**C2**
Average	3.93	4.41	4.36	4.22	4.84	3.99
Standard Deviation	0.39	0.61	0.68	0.82	1.04	0.55
t-test (p-value)	0.313		0.814		0.210	
	Ultimate Strain (mm/mm)					
Block	**A1**	**A2**	**B1**	**B2**	**C1**	**C2**
Average	0.0181	0.0186	0.0176	0.0201	0.0226	0.0212
Standard Deviation	0.0017	0.0027	0.0029	0.0034	0.0026	0.0018
t-test (p-value)	0.765		0.347		0.337	

Table 13: Compression test results by batch (dry specimens only).

	Modulus		
Batch	**A**	**B**	**C**
Avg	367	395	351
Std Dev	36.9	54.8	84.1
ANOVA		0.363	

	Yield Strength			Yield Strain		
Batch	**A**	**B**	**C**	**A**	**B**	**C**
Avg	3.75	3.77	3.85	0.0143	0.0134	0.0162
Std Dev	0.613	0.607	0.654	0.0026	0.0026	0.0035
ANOVA		0.939			0.157	

	Ultimate Stress			Ultimate Strain		
Batch	**A**	**B**	**C**	**A**	**B**	**C**
Avg	4.09	4.30	4.42	0.0183	0.0185	0.0219
Std Dev	0.497	0.677	0.861	0.0019	0.0031	0.0022
ANOVA		0.620			0.006	

The average modulus of all the dry specimens from all blocks was 369.11 MPa (σ = 65.05), and the average modulus of all the soaked specimens was 326.60 MPa (σ = 66.48). The moduli from the individual dry blocks ranged from 327 MPa to 417 MPa with the highest coefficient of variation in block C1 (COV = 30.9%) and the lowest COV in block B2 (COV = 7.1%). The moduli of the individual soaked blocks were found to range from 284 to 374 MPa. The highest COV was 24.7% found in block C2, and the lowest COV was 15.0% found in block A2.

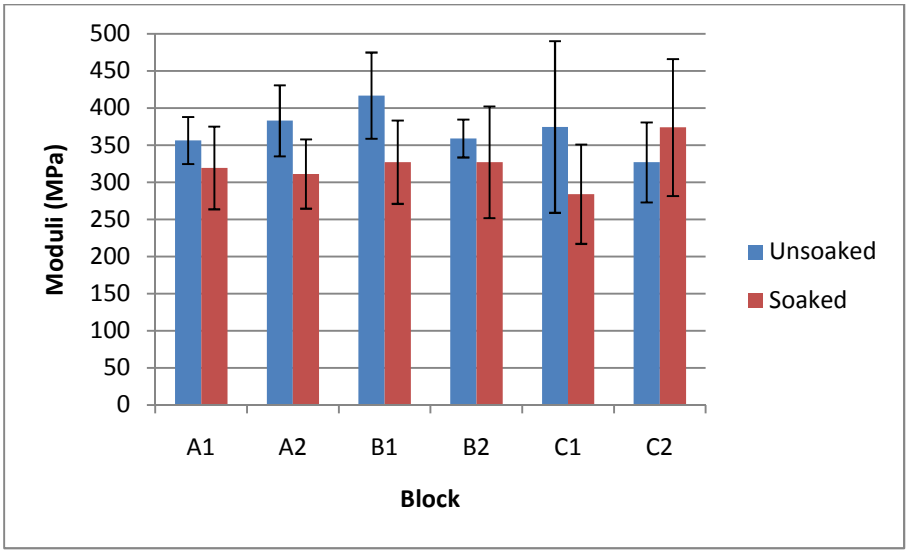

Figure 23: Average modulus of individual blocks with standard deviations. Blue bars are the untreated dry blocks; red bars are the soaked blocks.

The average yield stress of all the dry specimens was found to be 3.796 MPa (σ = 0.628); the average yield stress from all of the soaked specimens was 3.269 MPa (σ = 0.588). The maximum average yield stress in the dry blocks was seen in block A2 (4.208 MPa), and the minimum in block A1 (3.452 MPa). COVs in the dry blocks ranged from 11.9% (block A1) and 20.2% (block B2). The maximum average yield stress in the soaked blocks was 3.818 MPa in block C2; the minimum was found to be 2.965 MPa in block C1. The minimum COV was 10.5% in block A2; the maximum COV was 22.6% in block A1.

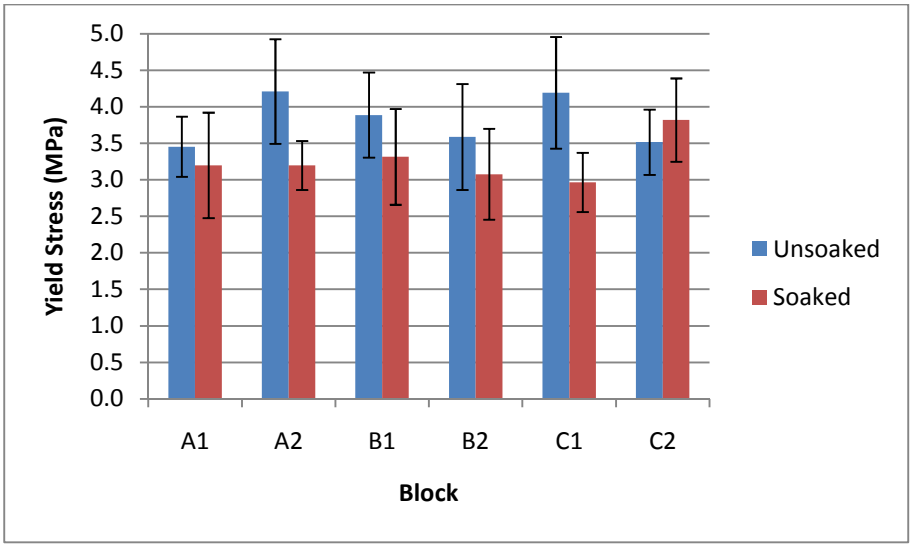

Figure 24: Average yield stress of individual blocks with standard deviations. Blue bars are the untreated dry blocks; red bars are the soaked blocks.

The average yield strain of all the dry specimens was 0.015 mm/mm (σ = 0.003), while the average of all soaked specimens was 0.014 mm/mm (σ = 0.003). This property showed the highest level of variation with the dry specimens having a COV of 21.6% and the dry specimens (most variation) having a COV of 23.5%. The average yield strain of the individual dry blocks ranged from 0.0133 (blocks A1 and B1) to 0.0168 mm/mm (block C1). The minimum and maximum COVs were found in the same blocks and varied between 15.8% and 27.5% (blocks A1 and C1 respectively). The average yield strain of the soaked blocks ranged from 0.0115 to 0.0156 mm/mm (blocks A1 and C1 respectively). The highest COV in the soaked blocks was found to be 30.9% in block C2; the lowest COV was 5.9% found in block A1.

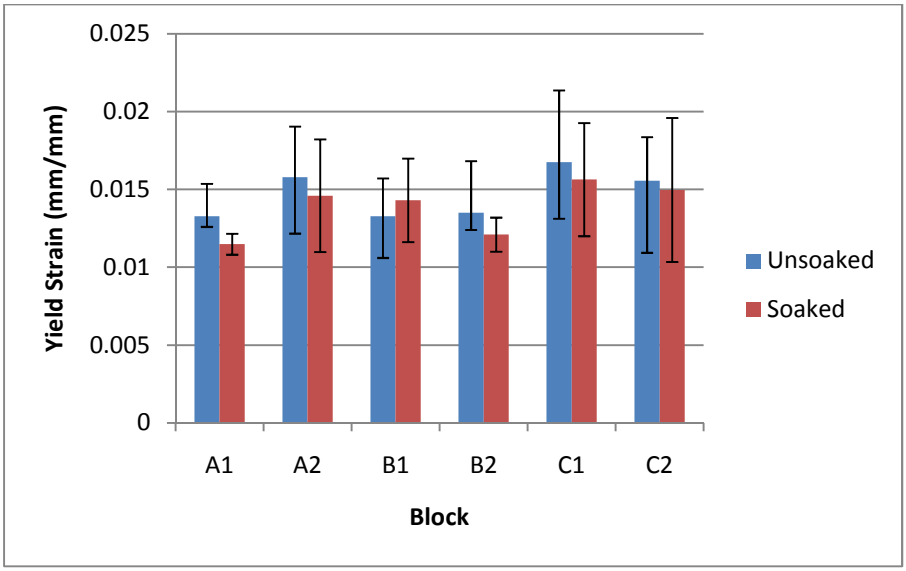

Figure 25: Average yield strain of individual blocks with standard deviations. Blue bars are the untreated dry blocks; red bars are the soaked blocks.

The average ultimate stress of all dry specimens was 4.274 MPa (σ = 0.710); the ultimate stress of all soaked specimens was 3.814 MPa (σ = 0.741). The maximum average ultimate stress in the dry blocks was seen in block C1 (4.843 MPa), and the minimum in block A1 (3.932 MPa). The maximum (21.6%) and minimum (10.0%) COVs of the dry blocks were also found in these blocks (blocks C1 and A1 respectively). In the soaked blocks, the maximum ultimate stress was 4.371 MPa in block C2, and the minimum ultimate stress was 3.447 MPa in block C1. The COVs in the soaked blocks varied from 12.5 to 26.1% (blocks A2 and A1 respectively).

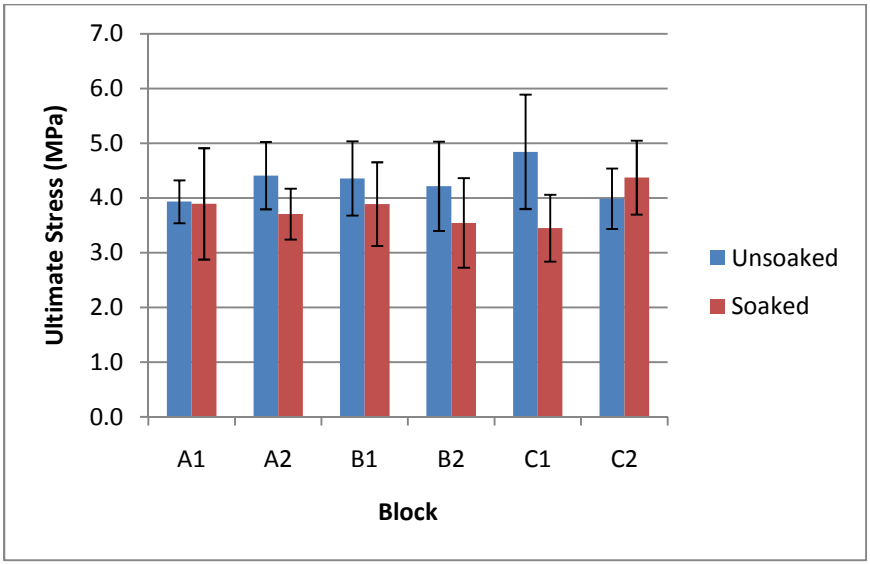

Figure 26: Average ultimate stress of individual blocks with standard deviations. Blue bars are the untreated dry blocks; red bars are the soaked blocks.

The average ultimate strain of all dry specimens was 0.0197 mm/mm (σ = 0.0029); the average ultimate strain of all soaked specimens was 0.0198 mm/mm (σ = 0.0030). The smallest amount of variation was seen in the dry specimens with a COV of 14.8% (absolute minimum), and the COV of the soaked specimens being 15.2%. The minimum average ultimate strain of the dry blocks was 0.0176 mm/mm in block B1. Block C1 had the highest average ultimate strain (0.0226 mm/mm) of the dry blocks. The COVs of the dry blocks ranged from 8.6% (block C2) to 16.8% (block B2). In the soaked blocks, the minimum ultimate strain was 0.0173 mm/mm (block B2), and the maximum ultimate strain was 0.0215 mm/mm (block C1). The COVs ranged from 7.0% (block B1) to 24.1% (block C2).

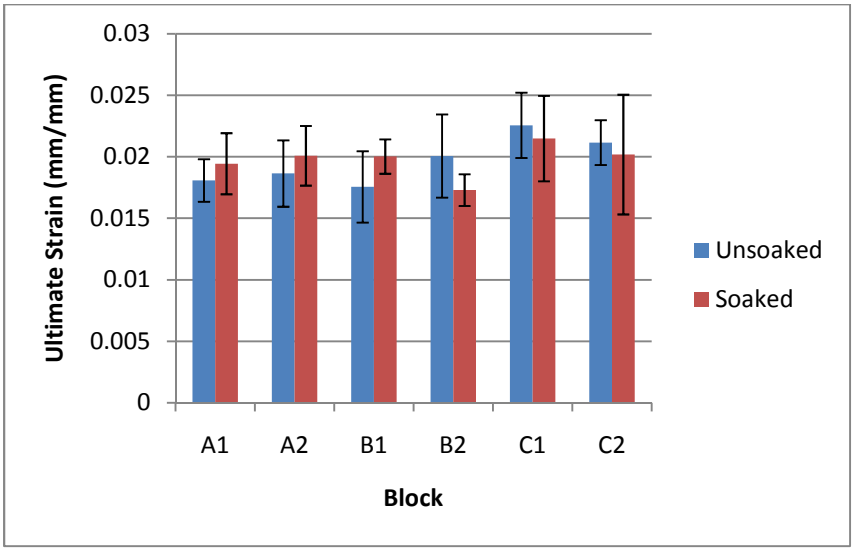

Figure 27: Average ultimate strain of individual blocks with standard deviations. Blue bars are the untreated dry blocks; red bars are the soaked blocks.

The modulus (p = 0.013), yield stress (p = 0.001), and ultimate stress (p = 0.017) all showed statistically significant differences between the dry and wet specimens when grouped by t-test analysis (α = 0.05). Yield strain (p = 0.386) and ultimate (p = 0.829) strain did not show any statistical difference by t-test analysis (α = 0.05).

3.3.2 Screw Pullout

The average pullout force of all dry specimens was 1199.3 N with a COV of 20.0%. The average pullout force of all soaked specimens was 978.7 N with a COV of 14.0%. Using the t-test (α = 0.05), a statistically significant difference was shown between the control (dry) and the treated (soaked) groups (p = 0.002). When comparing the dry versus soaked individual batches, there was no statistical difference, with the p-values from the t-test

ranging from 0.053 (batch A) to 0.152 (batch B); however, it is likely that there is a developing trend.

The highest average pullout force (1249.2 N) of the dry individual batches was seen in batch A; whereas, the highest average pullout force (1024.5 N) of the soaked individual batches was seen in block C. The highest amount of variation was also seen in these batches (dry batch A, COV = 25.0%; soaked batch C, COV = 16.4%).

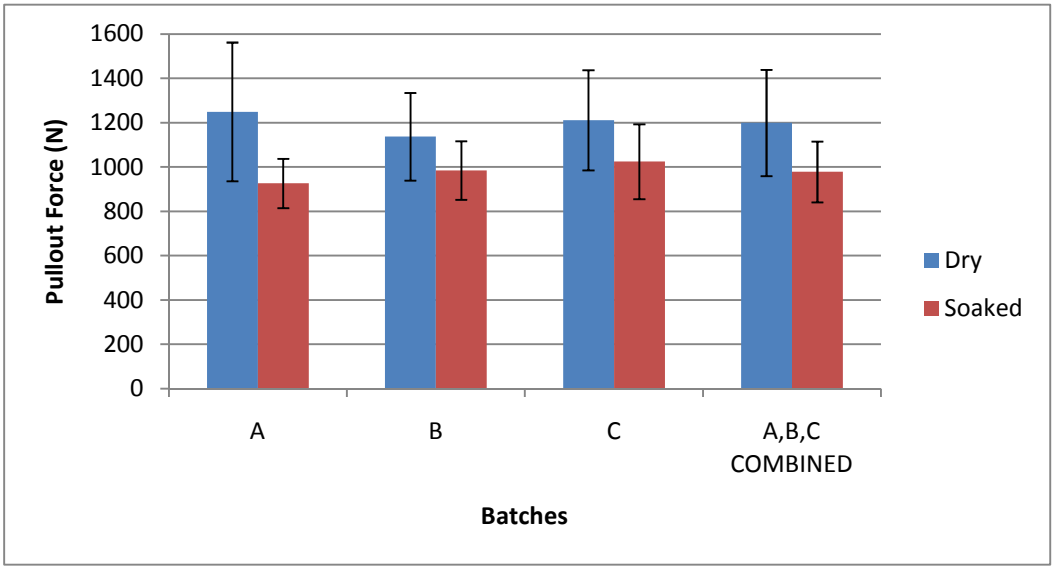

Figure 28: Average pullout force in bone screw pullout tests. Control (unsoaked) specimens are in blue; soaked specimens are in red.

Table 14: Screw pullout test results by batch and grouped.

Screw Pullout Results								
	A		B		C		ALL BLOCKS	
	Dry	Soaked	Dry	Soaked	Dry	Soaked	Dry	Soaked
Average Pullout Force (N)	1249	927	1137	985	1212	1025	1199	979
Standard Deviation	313	111	198	132	226	168	240	137
COV	25.0%	12.0%	17.4%	13.4%	18.7%	16.4%	20.0%	14.0%
p-value from t-test	0.053		0.152		0.138		0.0022	

3.5 Discussion

3.5.1 Compression

After comparing blocks and batches to show the manufacturing process does not produce a significant variation in these properties by compression testing, it was determined that all samples could be grouped together to explore the effect of the synthetic marrow. This also shows the manufacturing process of the synthetic cancellous foam is reliable and repeatable as is necessary for the production of the Analogue Spine Model.

The average modulus of all the dry and soaked specimens was found to be 369 and 327 MPa with coefficients of variation (COV) of 17.6% and 20.4%, respectively. Statistical tests showed a significant difference between the data ($p = 0.01$, $\alpha = 0.05$), proving that the synthetic marrow had an effect on the modulus of the synthetic bone. The decrease in the value of the modulus increases its acceptability to use as a substitute for cancellous bone. The average found for the dry specimens (369 MPa) is slightly higher than reported in literature (290 – 350 MPa) [34-35], whereas the value reported for the soaked specimens

(327 MPa), as would be found in the model, was within the range of accepted values for human vertebral cancellous bone.

The variation seen in the samples was relatively low when compared with values of human vertebral cancellous bone. The standard deviations seen in both the dry and soaked samples (65.1 and 66.5 MPa, respectively) were very close in value, both of which were much lower than the values reported in literature (113 – 145 MPa, Table 14) for similar boundary conditions [34-35]. In addition, the minimum and maximum values of moduli bracketed a smaller range than in the literature (192 – 456 MPa, soaked, experimental; 90 – 725 MPa, literature) [34-35]. This demonstrates the synthetic vertebral cancellous bone has less variability than its human counterpart.

Table 15: Test results and literature values for the moduli of analogue and vertebral cancellous bone.

Author	Year	Boundary Condition	Avg	Std Dev	Min	Max
Current Study (dry)	*2011*	*Capped*	*369*	*66.1*	*176*	*485*
Current Study (soaked)	*2011*	*Capped*	*327*	*66.5*	*192*	*456*
Banse [35]	2002	Capped	352	145	127	725
Morgan / Keaveny [36]	2002	Capped	344	148	---	---
Kopperdahl / Keaveny [34]	1998	Capped	291	113	90	536
Moseklide [37]	1987	Platen	67	7	---	---
Hou [32]	1998	Platen	316	226	10.6	975.6
Lindahl [38]	1976	Platen	55.6	0.7	1.1	139

Modulus of elasticity is the most vital property when considering the spine model. The model will be designed to be used in testing of physiological loads on the spine. These loads would occur before the cancellous bone would begin to yield or fail. However, it is important to obtain a more complete understanding of the material in question; therefore, the yield stress and strain were also calculated.

The yield stress of the dry specimens was found to be 3.796 MPa; the average yield stress observed of the soaked specimens was significantly lower at 3.269 MPa. Similar to modulus, the magnitude of the property was decreased in the soaked specimens, however,

this improves the candidacy of the material. The reported range for yield stress of human vertebral cancellous bone is 1.92 – 2.02 MPa in studies with similar boundary conditions [34, 36]. Other studies report yield stress to be as high as 4 MPa [38]. The application of marrow decreased the measure of yield stress to better model human bone. The standard deviation in yield stress of the dry and soaked specimens (0.628 and 0.588 MPa, respectively) are approximately one-third of the values reported in the literature (0.84 – 0.92 MPa) [34, 36]. This demonstrates better reproducibility of results, with smaller variation of properties than seen in cadaver specimens.

Table 16: Test results and literature values for the yield stress of analogue and vertebral cancellous bone.

Author	Year	Boundary Condition	Avg	Std Dev	Min	Max
Current Study (dry)	*2011*	*Capped*	*3.80*	*0.628*	*2.80*	*5.11*
Current Study (soaked)	*2011*	*Capped*	*3.27*	*0.588*	*2.20*	*4.40*
Morgan / Keaveny [36]	2002	Capped	2.02	0.92	---	---
Kopperdahl / Keaveny [34]	1998	Capped	1.92	0.84	0.56	3.71
Lindahl [38]	1976	Platen	4	0.1	0.1	9.7

Yield strain was one of two properties that did not show a statistically significant change in value between the dry and soaked specimens. The values from the current study compare favorably to the values reported in literature. The average value for yield strain is

slightly higher but still in the range of those in Table 16. The standard deviation of the synthetic trabecular bone is higher than those reported in Table 16. This could be due in part to the measurement of the deflection of the specimens in the current study. The deflection measured was the displacement of the loading platens. A source of error can arise from using this measurement due to testing artifacts from the capping of specimens. To establish true strain, an extensometer should be used to measure deflection of the material only. No such instrument was available, and with the limitations inherent to product development, mainly time and budget limitations, acquiring an extensometer was not a feasible option.

Table 17: Test results and literature values for the yield strain of analogue and vertebral cancellous bone.

Author	**Year**	**Boundary Condition**	**Avg** (%)	**Std Dev** (%)	**Min** (%)	**Max** (%)
Current Study (dry)	*2011*	*Capped*	*1.47*	*0.30*	*0.98*	*2.45*
Current Study (soaked)	*2011*	*Capped*	*1.40*	*0.30*	*0.92*	*2.33*
Morgan / Keaveny [36]	2002	Capped	0.77	0.06	---	---
Kopperdahl / Keaveny [34]	1998	Capped	0.84	0.06	0.75	0.95
Lindahl [38]	1976	Platen	6.7	0.2	4.1	8.60

Ultimate stress and strain, though not as critical as modulus, is still an important factor in the evaluation of the material in question. While the ASM is not intended for

testing at such extreme levels, from a product design position, it is important to understand the materials used in the design. As with many products, users may test the boundaries of the intended function of the ASM.

The ultimate stress values (4.27 MPa, dry; 3.81 MPa, soaked) found for the synthetic cancellous bone were found to be slightly higher than seen in values reported in literature for human vertebral cancellous bone test using similar boundary conditions (2.23 - 2.37 MPa) but still in the range of other reports (2.23 – 4.6 MPa) [34, 35, 38]. This property did show a statistically significant difference between the two conditions; however, the effect lowered the value of ultimate stress to better match values from the literature. The standard deviation (0.741 MPa) and the range of minimum and maximum values (2.44, 5.05 MPa) were both lower in the soaked samples than reported in literature (0.95, 1.14 MPa, standard deviation; 0.6, 6.17 MPa, minimum, maximum) [34, 35], demonstrating better precision of the material.

Table 18: Test results and literature values for the ultimate stress of analogue and vertebral cancellous bone.

Author	Year	Boundary Condition	Avg	Std Dev	Min	Max
Current Study (dry)	*2011*	*Capped*	*4.27*	*0.710*	*3.14*	*5.87*
Current Study (soaked)	*2011*	*Capped*	*3.81*	*0.741*	*2.44*	*5.05*
Banse [35]	2002	Capped	2.37	1.14	0.6	6.17
Kopperdahl / Keaveny [34]	1998	Capped	2.23	0.95	0.7	4.33
Moseklide [37]	1987	Platen	2.45	0.24	---	---
Hou [32]	1998	Platen	3.29	2.34	---	---
Lindahl [38]	1976	Platen	4.6	0.3	0.2	10.5

Ultimate strain values were within the range reported in literature and found in Table 18. Standard deviations from the study were also very similar to those found in the literature. It should be noted once more that the deflection used to calculate ultimate strain was the displacement of the loading platens, which can introduce error due to testing artifacts that can arise from capping the ends of the specimens.

Table 19: Test results and literature values for the yield strain of analogue and vertebral cancellous bone.

Author	**Year**	**Boundary Condition**	**Avg** (%)	**Std Dev** (%)	**Min** (%)	**Max** (%)
Current Study (dry)	*2011*	*Capped*	*1.97*	*0.29*	*1.53*	*2.61*
Current Study (soaked)	*2011*	*Capped*	*1.98*	*0.30*	*1.43*	*2.89*
Banse [35]	2002	Capped	1.19	0.26	0.72	2.01
Kopperdahl / Keaveny [34]	1998	Capped	1.45	0.33	0.96	2.30
Moseklide [37]	1987	Platen	7.40	0.20	---	---
Lindahl [38]	1976	Platen	9.50	0.40	5.30	1.44

The data analysis showed the synthetic marrow altered the material properties enough to be statistically significant. However, as mentioned, the changes in material properties were constructive, as the properties were altered in a way that made the analogue cancellous bone a better match for vertebral cancellous bone. The properties better matched the reported values in literature for vertebral cancellous bone. The effect of the marrow failed to significantly alter the standard deviations of the properties, thus the materials precision remained intact. This is important as a major goal of the ASM is consistency and precision of the mechanical properties.

These changes may have been due to the synthetic marrow plasticizing the material. This conclusion may be drawn due to the lowering of stiffness, yield stress, and ultimate stress and the lowering of yield strain and ultimate strain.

3.5.2 Screw Pullout

Screw pullout data is difficult to compare to values in literature. Ultimate pullout force is highly dependent on the following:

1. Screw type – screw diameter, pitch, angle of threads, screw profile, metallic or resorbable
2. Depth of insertion
3. Type of bone – presence and/or thickness of cortical shell, bone mineral density, and location of bone
4. Insertion torque
5. Rate of pullout

With this in mind, Table 20 shows literature values for screw pullout strength. As with other mechanical properties of cancellous bone, pullout strength varies significantly. Reported values for pullout strength of cancellous bone range from 678 to 3224 N [70] [71]. Values for other foams used in bone screw testing reported in the table fall within this range, as does the current study. Standard deviations in the study fall within the range of those reported for cancellous bone.

Table 20: Test results and literature values for the pullout strength of analogue and cancellous bone.
[1] Tapered inner diameter
[2] Limited information on screw type
[3] Estimate from plot
[4] Independent lab analysis for Sawbones closed-cell foam

Author(s)	Year	Screw Description	Specimen Description	Insertion Depth (mm)	Rate of Pullout (mm/s)	Pullout Strength (N)	Standard Deviation
Current Study (no soak)	2011	od = 6.4 mm id = 4.0 mm[1] TPI = 9.2	32 lb/ft^3 open-cell foam	20	0.08	1199	240
Current Study (2 wk soak)	2011	od = 6.4 mm id = 4.0 mm[1] TPI = 9.2	32 lb/ft^3 open-cell foam	20	0.08	979	137
Pfeiffer / Abernathie [72]	2006	Pioneer, 6.75 mm[1,2] TPI = 9	20 lb/ft^3 closed-cell foam	---	0.085	2400[3]	
Asnis, et al. [73]	1996	od = 6.4 mm id = 4.2 mm[1] TPI = 14	closed cell (pedilen) 13.7 lb/ft^3	19	0.1 (pushout)	725[3]	---
Mermelstein, et al. [70]	1996	cancellous 4.0 mm, Synthes	canine, femoral, trabecular	19	0.08	678	297
Tingart, et al. [74]	2006	cancellous 6.5 mm, Synthes	human, humeral, trabecular	23.4	0.1 cyclic to load (100 N to 800 N)	738	220
General Plastics[4] [75]	2009	od = 4.5 mm id = 3.0 mm TPI = 14.5	20 lb/ft^3 Sawbones closed-cell foam	25.4	0.08	968.4	25.2
Finlay, et al. [71]	1989	od = 6.5 mm id = 3.0 mm TPI = 9.2	bovine, vertebral, trabecular	15	0.2	3224	400[3]

3.6 Conclusion

The study results showed the foam was significantly affected by exposure to the synthetic marrow. Modulus, yield stress, ultimate stress, and pullout strength were all found to be significantly altered after four weeks of soaking in the synthetic marrow. Yield and ultimate strain were the only two properties measured that showed no significant change. All of the changes to the properties were in a direction that made the analogue bone a better mechanical match for vertebral cancellous bone.

While the changes in the properties were advantageous, further testing should completed to ensure the properties do not continue to deteriorate. Samples should be soaked for longer durations and tested in the same manner. In addition, an extensometer should be used to measure yield and ultimate strain.

This study did also not account for age changes in the material. In future testing, in addition to control and soaked groups, an untreated group should be allowed to age for the same amount of time as the soaked group to test for age changes.

This study only measured the effect of marrow on the foam used to model cancellous bone. In the ASM, the cortical substitute will also be exposed to the synthetic marrow, thus, should be tested in a similar manner to determine the effects of the synthetic marrow on the cortical bone substitute. Future testing should also include the entire vertebrae to determine how the synthetic marrow will respond to testing. A vertebrae filled with the synthetic marrow may hydraulic stiffen upon compression. Further testing can determine these effects.

Chapter 4: Conclusions and Future Work

4.1 Conclusions and Future Work

From the studies presented, the synthetic marrow had a significant impact on the material properties of the analogue cancellous bone. The four-point bending tests showed that the resins used to produce analogue bone were susceptible to change after soaking in the synthetic marrow. The resin used to manufacture analogue cancellous bone exhibited significant change in modulus, which was the only property reported. This was confirmed in compression tests of the analogue cancellous bone. Modulus, yield stress, ultimate stress, and pullout strength were all found to be significantly altered after four weeks of soaking in the synthetic marrow. Yield and ultimate strain were the only two properties measured that showed no significant change. While the mechanical properties were affected by the synthetic marrow, they were affected in an advantageous way. All properties were changed in a way that made the analogue cancellous bone a more suitable mechanical match for vertebral cancellous bone after 4 weeks of soaking in the synthetic marrow; however, it is unknown if the properties will continue to decreases during longer soaking durations. The results still compared well with values from literature in every property measured. However, further testing should completed to ensure the properties affected by the four week soak do not continue to deteriorate in longer soaking durations. In addition, an extensometer should be used to measure strains in the test specimens.

The exact cause and mechanism of the change in material properties due to the four week exposure to the synthetic bone marrow is not clear. A possible hypothesis is that the synthetic marrow plasticized the analogue bone and the resins used to make the same. If

this is accurate, longer soaking durations could result in a further decrease in the material properties. This should be evaluated by future testing.

One concern of filling vertebrae with synthetic marrow is the effect of hydrostatic pressure on mechanical testing. Human cortical bone (and vertebral endplates) is somewhat porous and can allow for marrow escape when subjected to loads whereas they analogue model does not have a porous cortical shell. This could lead to substantial hydrostatic forces from within the vertebrae.

Other future tests should include entire vertebrae filled with marrow and tested in various modes such as compression, screw pullout (with and without cement augmentation), cement intrusion, and screw toggle. The vertebrae should also be filled with marrow to different pressures to see what effect this has on the mechanical properties.

References

[1] F. H. Martini, M. J. Timmons and R. B. Tallitsch, Human Anatomy, 4th ed., Upper Saddle River, New Jersey: Pretince Hall, 2003.

[2] S. M. Kurtz and A. A. Edidin, Spine Technology Handbook, London: Academic Press Inc., 2006.

[3] M. J. Silva, C. Wang, T. Keaveny and W. Hayes, "Direct and computed tomography thickness measurements of the human lumbar vertebral shell and endplate," *Bone,* vol. 15, pp. 409-414, 1994.

[4] T. W. Edwards, Y. Zheng, L. A. Ferrara and J. A. Hansen, "Structural Features and Thickness of the Vertebral Cortex in the Thoracolumbar Spine," *Spine,* vol. 26, no. 2, pp. 218-222, 2001.

[5] National Cancer Institue, "SEER Traning," [Online]. Available: http://training.seer.cancer.gov/anatomy/skeletal/tissue.html.

[6] S. K. Eswaran, A. Gupta, M. F. Adams and T. M. Keaveny, "Cortical and trabecular load sharing in the human vertebral body," *Journal of Bone and Mineral Research,* vol. 21, no. 2, pp. 307-314, November 2005.

[7] M. Nissan and I. Gilad, "The cervical and lumbar vertebrae an anthropometric model," *Engineering in Medicine,* vol. 13, pp. 111-114, 1984.

[8] H. Kugel, C. Jung, O. Schulte and W. Heindel, "Age- and sex-specific differences in the 1H-spectrum of vertebral bone marrow," *J. Magnetic Resonance Imaging,* vol. 13, no. 2, pp. 263-268, February 2001.

[9] I. Gilad and M. Nissan, "Sagittal evaluation of elemental geometrical dimensions of human vertebrae," *Journal of Anatomy,* vol. 143, pp. 115-120, 1985.

[10] R. McBroom, W. Hayes, R. Goldberg and A. 3. White, "Prediction of vertebral body compressive fracture using quantitative computed tomography," *J Bone Joint Surg Am,* vol. 67, no. 8, pp. 1206-1214, 1985.

[11] D. S. Rockoff, E. Sweet and J. Bleustein, "The relative contribution of trabecular and cortical bone to the strength of human lumbar

vertebrae," *Calcified Tissue International,* vol. 3, no. 1, pp. 163-175, 1969.

[12] M. J. Silva, T. M. Keaveny and W. C. Hayes, "Load Sharing Between the Shell and Centrum in the Lumbar Vertebral Body," *Spine,* vol. 22, no. 2, pp. 140-150, 1997.

[13] S. J. Ferguson and T. Steffen, "Biomechanics of the aging spine," *European Spine Journal,* vol. 12, no. 0, pp. s97-s103, 2003.

[14] M. R. Rubin and J. P. Bilezikian, "SciELO Brazil," [Online]. Available: http://www.scielo.br/scielo.php?script=sci_arttext&pid=S0004-27302010000200019.

[15] S. Cowin and J. Telega, "Bone Mechanics Handbook," in *Applied Mechanics Reviews*, vol. 56, 2003, pp. B61-B63.

[16] T. H. Smit, A. Odgaard and E. Schneider, "Structure and function of vertebrae trabecular bone," *Spine,* vol. 22, no. 24, pp. 2823-2833, 1997.

[17] H. Roesler, "Some historical remarks on the theory of cancellous bone structure (Wolff's law)," in *Mechanical Properties of Bone*, New York: The American Society of Mechanical Engineers, 1981, pp. 27-42.

[18] R. Muller, "Springer Images," [Online]. Available: http://www.springerimages.com/.

[19] L. G. Raisz, "Physiology and pathophysiology of bone remodeling," *Clinical Chemistry,* vol. 45, pp. 1353-1358, 1999.

[20] V. Tzelepi, A. C. Tsamandas, V. Zolota and C. D. Scopa, "Bone anatomy, physiology and function," in *Bone Metastases*, vol. 12, Springer Netherlands, 2009, pp. 3-30.

[21] U. A. Gurkan and O. Akkus, "The mechanical environment of bone marrow: a review," *Annals of Biomedical Engineering,* vol. 36, no. 12, pp. 1978-1991, December 2008.

[22] N. Shaw, "Studies on intramedullary pressure and blood flow in bone," *American Heart Journal,* vol. 68, pp. 134-135, July 1964.

[23] R. S. Ochia and R. P. Ching, "Rate dependence of hydraulic resistance in human lumbar vertebral bodies," *Spine,* vol. 31, no. 22, pp. 2569-2574, October 2006.

[24] M. Kasra and M. D. Grynpas, "On shear properties of trabecular bone under torsional loading: Effects of bone marrow and strain rate," *Journal of Biomechanics,* vol. 40, no. 13, pp. 2898-2903, 2007.

[25] R. S. Ochia and R. P. Ching, "Hydraulic resistance and permeability in human lumbar vertebral bodies," *j. Biomech. Eng.,* vol. 124, no. 5, pp. 533-537, October 2002.

[26] N. Shaw, "Observations on the intramedullary blood-flow and marrow-pressure in bone," *Clinical Science,* vol. 24, pp. 311-318, June 1963.

[27] B. L. Davis and S. S. Praveen, "Nonlinear versus linear behavior of calcaneal bone marrow at different shear rates," in *American Society of Biomechanics*, Blacksburg, VA, 2006.

[28] Y. Eguhi and T. Karino, "Measurement of rheologic property of blood by a falling-ball blood viscometer," *Annals of Biomedical Engineering,* vol. 36, no. 4, pp. 545-553, April 2008.

[29] U. A. Gurkan and O. Akkus, "An implantable magnetoelastic sensor system for wireless physiological sensing of viscosity," in *Proceeding of the ASME Summer Bioengineering Conference*, New York, 2007.

[30] D. R. White, H. Q. Woodard and S. M. Hammond, "Average soft-tissue and bone models for use in radiation dosimetry," *British Journal of Radiology,* vol. 60, pp. 907-913, 1987.

[31] R. Heaney, "The natural history of vertebral osteoporosis. Is low bone mass an epiphenomenon?," *Spine,* vol. 13, no. 2, pp. s23-226, 1992.

[32] F. J. Hou, S. M. Lang, D. A. Reimann and D. P. Fyhrie, "Human vertebral body apparent and hard tissue stiffness," *Journal of Biomechanics,* vol. 31, no. 11, pp. 1009-1015, November 1998.

[33] F. Linde, I. Hvid and F. Madsen, "The effect of specimen geometry on the mechanical behaviour of trabecular bone specimens," *Journal of Biomechanics,* vol. 25, no. 4, pp. 359-368, 1992.

[34] D. Kopperdahl and T. Keaveny, "Yield strain behavior of trabecular bone," *Journal of Biomechanics,* vol. 31, pp. 601-608, 1998.

[35] X. Banse, T. Sims and A. Bailey, "Mechanical properties of adult vertebral cancellous bone: correlation with collagen intermolecular cross-links,"

Journal of Bone and Mineral Research, vol. 17, no. 9, pp. 1621-1628, 2002.

[36] E. Morgan and T. Keaveny, "Dependence of yield strain of human trabecular bone on anatomic site," *Journal of Biomechanics,* vol. 34, no. 5, p. 569, 2001.

[37] L. Mosekilde, L. Mosekilde and C. Danielsen, "Biomechanical competence of vertebral trabecular bone in relation to ash density and age in normal individuals," *Bone,* vol. 8, no. 2, pp. 79-85, 1987.

[38] O. Lindahl, "Mechanical properties of dried defatted spongy bone," *Acta Orthopaedica,* vol. 47, no. 1, pp. 11-19, 1976.

[39] A. L. Nachemson, A. B. Schultz and M. H. Berkson, "Mechanical Properties of Human Lumbar Spine Motion Segments: Influences of Age, Sex, Disc Level, and Degeneration," *Spine,* vol. 4, no. 1, January/February 1979.

[40] H.-J. Wilke, K. Wenger and L. Claes, "Testing criteria for spinal implants: recommendations for the standardization of in vitro stability testing of spinal implants," *European Spine Journal,* vol. 7, no. 2, pp. 148-154, 1998.

[41] A. L. Anderson, T. E. McIff, M. A. Asher, D. C. Burton and C. R. Glattes, "The effect of posterior thoracic spine anatomical structures on motion segment flexion stiffness," *Spine,* vol. 34, no. 5, pp. 441-446, March 2009.

[42] H.-J. Wilke, B. Jungkunz, K. Wenger and L. E. Claes, "Spinal segment range of motion as a function of in vitro test conditions: Effects of exposure period, accumulated cycles, angular-deformation rate, and moisture condition," *The Anatomical Record,* vol. 251, no. 1, pp. 15-19, May 1998.

[43] M. Hongo, R. E. Gay, J.-T. Hsu, K. D. Zhao, B. Illharreborde, L. J. Berglund and K.-N. An, "Effect of multiple freeze–thaw cycles on intervertebral dynamic motion characteristics in the porcine lumbar spine," *Journal of Biomechanics,* vol. 41, no. 4, pp. 916-920, 2008.

[44] M. Shea, W. Edwards, A. White and W. Hayes, "Variations of stiffness and strength along the human cervical spine," *Journal of Biomechanics,* vol. 24, no. 2, pp. 95-97, 99-107, 1991.

[45] R. F. McLain, S. A. Yerby and T. A. Moseley, "Comparative morphometry of L4 vertebrae: comparison of large animal models for the human lumbar spine," *Spine,* vol. 27, no. 8, pp. E200-E206, April 2002.

[46] B. W. Cunningham, Y. Kotani, P. S. McNulty, A. Cappuccino and P. C.

McAfee, "The effect of spinal destabilization and instrumentation on lumbar intradiscal pressure: an in vitro biomechanical analysis," *Spine,* vol. 22, no. 22, pp. 2655-2663, November 1997.

[47] ASTM, *F2077-03 - Test Methods for Intervertebral Body Fusion Devices.*

[48] "Shanghai E-Feature Information Technology," [Online]. Available: http://www.e-feature.net/en/content/fea.

[49] J. Domann, "Development and Validation of an Analogue Lumbar Spine Model and its Integral Components," Lawrence, 2011.

[50] E. Friis, C. Pence, C. Graber and J. Montoya, "Mechanical analogue model of the human lumbar spine: development and initial evaluation," in *Spinal Implants: Are We Evaluating Them Appropriately?*, ASTM Int., 2003.

[51] Domann JP, Friis EA, Mar D, Johnson A, James J: The Analogue Spine Model: The First Anatomically and Mechanically Correct Synthetic Physical Model of the Lumbar Spine, North American Spine Society, November 2011.

[52] L.-H. Chen, C.-L. Tai, P.-L. Lai, L. De-Mei, T.-T. Tsai, T.-S. Fu, C.-C. Niu and W.-J. Chen, "Pullout strength for cannulated pedicle screws with bone cement augmentation in severely osteoporotic bone: Influences of radial hole and pilot hole tapping," *Clinical Biomechanics,* vol. 24, no. 8, pp. 613-618, October 2009.

[53] F. Miller and A. Johnson, "Artificial Bones and Methods of Making Same". United States Patent 20,090/216,327, 2008.

[54] L. LaPierre, *Control of the mechanical properties of the synthetic anterior longitudinal ligament and its effect on the mechanical analogue lumbar spine model,* D. o. M. Engineering, Ed., Lawrence, KS: University of Kansas, 2009, p. 152.

[55] C. Hirsch, "The reaction of intervertebral discs to compression forces," *Jour. Bone Joint Surg.,* vol. 37, no. 6, pp. 1188-1196, 1955.

[56] K. Markolf, "Deformation of the thoracolumbar intervertebral joints in response to external loads: a biomechanical study using autopsy material," *Jour. Bone Joint Surg. Am.,* vol. 54, no. 3, pp. 511-533, April 1972.

[57] R. Majkowski, A. Miles, G. Bannister, J. Perkins and G. Taylor, "Bone surface preparation in cemented joint replacement," *J. Bone Joint Surg.,* Vols. 75-B, no. 3, pp. 459-463, 1993.

[58] R. Majkowski, G. Bannister and A. Miles, "The effect of bleeding on the cement-bone interface," *Clinical Orthopaedics and Related Research,* vol. 299, pp. 293-297, 1994.

[59] ASTM, *D6272 - 10 Standard Test Method for Flexural Properties of Unreinforced and Reinforced Plastics and Electrical Insulating Materials by Four-Point Bending.*

[60] J.-Y. Rho, L. Kuhn-Spearing and P. Zioupos, "Mechanical properties and the hierarchical structure of bone," *Medical Engineering and Physics,* vol. 20, no. 2, pp. 92-102, March 1998.

[61] K. Choi and S. Goldstein, "A comparison of the fatigue behavior of human trabecular and cortical bone tissue," *Journal of Biomechanics,* vol. 25, no. 12, pp. 1371-1381, December 1992.

[62] J. Kuhn, S. Goldstein, R. Choi, M. London, L. Feldkamp and L. Matthews, "Comparison of the trabecular and cortical tissue moduli from human iliac crests," *Journal of Orthopaedic Research,* vol. 7, no. 6, pp. 876-884, November 1989.

[63] S. D. Ryan and J. L. Williams, "Tensile testing of rodlike trabeculae excised from bovine femoral bone," *Journal of Biomechanics,* vol. 22, no. 4, pp. 351-355, 1989.

[64] K. Choi, J. Kuhn, M. Ciarelli and S. Goldstein, "The elastic moduli of human subchondral, trabecular, and cortical bone tissue and the size-dependency of cortical bone modulus," *Journal of Biomechanics,* vol. 23, no. 11, pp. 1103-1113, 1990.

[65] J. Y. Rho, R. B. Ashman and C. H. Turner, "Young's modulus of trabecular and cortical bone material: Ultrasonic and microtensile measurements," *Journal of Biomechanics,* vol. 26, no. 2, pp. 111-119, February 1993.

[66] C. H. Turner, J. Rho, Y. Takano, T. Y. Tsui and G. M. Pharr, "The elastic properties of trabecular and cortical bone tissues are similar: results from two microscopic measurement techniques," *Journal of Biomechanics,* vol. 32, no. 4, pp. 437-441, April 1999.

[67] J. Yang and R. S. Lakes, "Experimental study of micropolar and couple stress elasticity in compact bone in bending," *Journal of Biomechanics,* vol. 15, no. 2, pp. 91-98, 1982.

[68] ASTM, *D1621-04 Standard Test Method for Compressive Properties Of Rigid Cellular Plastics.*

[69] ASTM, *F1839 - 08e1 Standard Specification for Rigid Polyurethane Foam for Use as a Standard Material for Testing Orthopedic Devices and Instruments.*

[70] L. Mermelstein, L. Chow, C. Friedman and J. Crisco III, "The reinforcement of cancellous bone screws with calcium phosphate cement," *Journal of Ortho Trauma,* vol. 10, no. 1, pp. 15-20, January 1996.

[71] B. J. Finlay, I. Harada, R. B. Bourne, C. H. Rorabeck, R. Hardie and M. A. Scott, "Analysis of the pull-out strength of screws and pegs used to secure tibial components following total knee arthroplasty," *Clinical Orthopaedics & Related Research,* vol. 247, pp. 220-231, October 1989.

[72] F. M. Pfeiffer and D. L. Abernathie, "A comparison of pullout strength for pedicle screws of different designs: A study using tapped and untapped pilot holes," *Spine,* vol. 31, no. 23, pp. E867-E870, November 2006.

[73] S. E. Asnis, J. J. Ernberg, M. P. Bostrom, T. M. Wright, R. M. Harrington, A. Tencer and M. Peterson, "Cancellous bone screw thread design and holding power," *Journal of Orthopaedic Trauma,* vol. 10, no. 7, pp. 462-469, October 1996.

[74] M. J. Tingart, J. Lehtinen, D. Zurakowski, J. J. Warner and M. Apreleva, "Proximal humeral fractures: Regional differences in bone mineral density of the humeral head affect the fixation strength of cancellous screws," *Journal of Shoulder and Elbow Surgery,* vol. 15, no. 5, pp. 620-624, 2006.

[75] General Plastics Manufacturing Company, *Independent lab analysis of Sawbones closed-cell foam by General Plastics,* Bun # 072808-08 ed., Vols. FR-6715, Jerry, Ed., Tacoma, WA, 2009.

[76] J. Harms, "Harms' Spine Surgery," [Online]. Available: http://harms-spinesurgery.com/.

[77] M. Aebi, "Springer Images," [Online]. Available:

http://www.springerimages.com/.

Appendix A: Four-point Bend Test Results

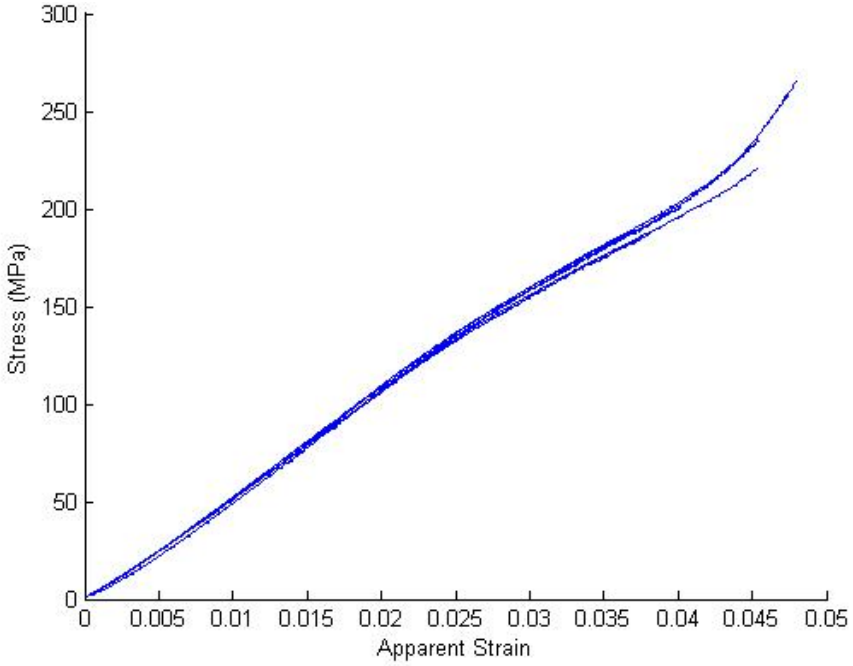

Figure 29: Stress-strain curves for samples 1-6, material A, control (no soak).

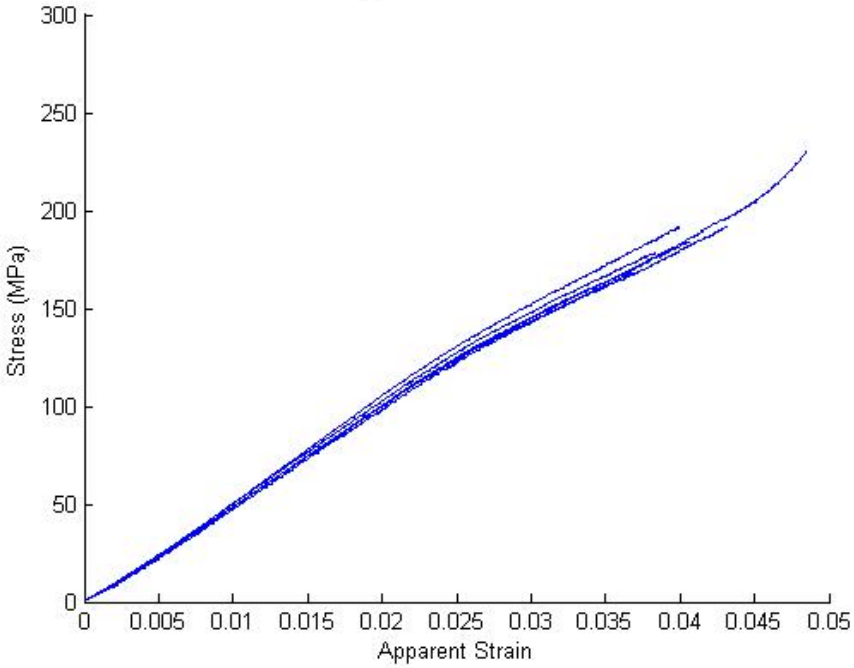

Figure 30: Stress-strain curves for samples 1-6, material A, 2-week soak.

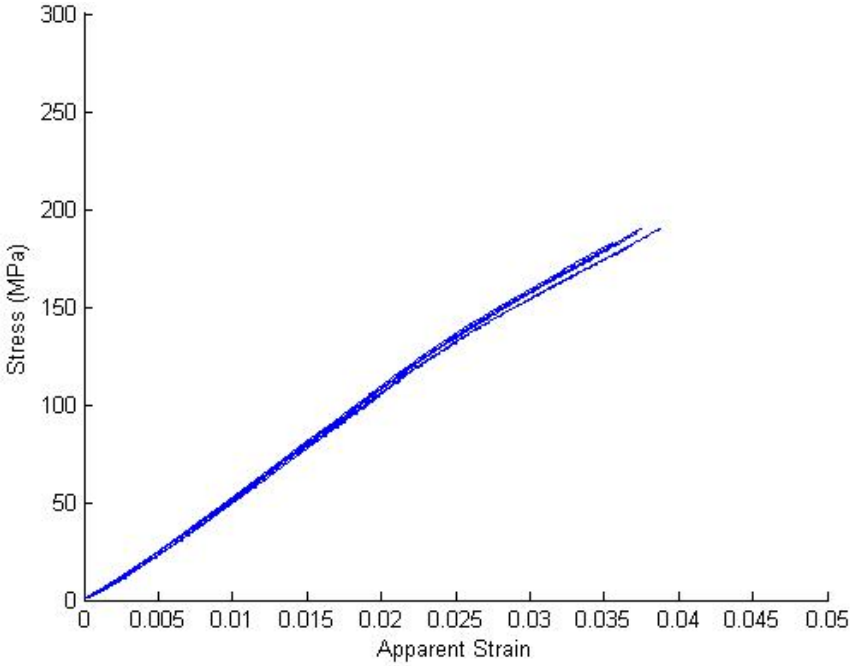

Figure 31: Stress-strain curves for samples 1-6, material A, 4-week soak.

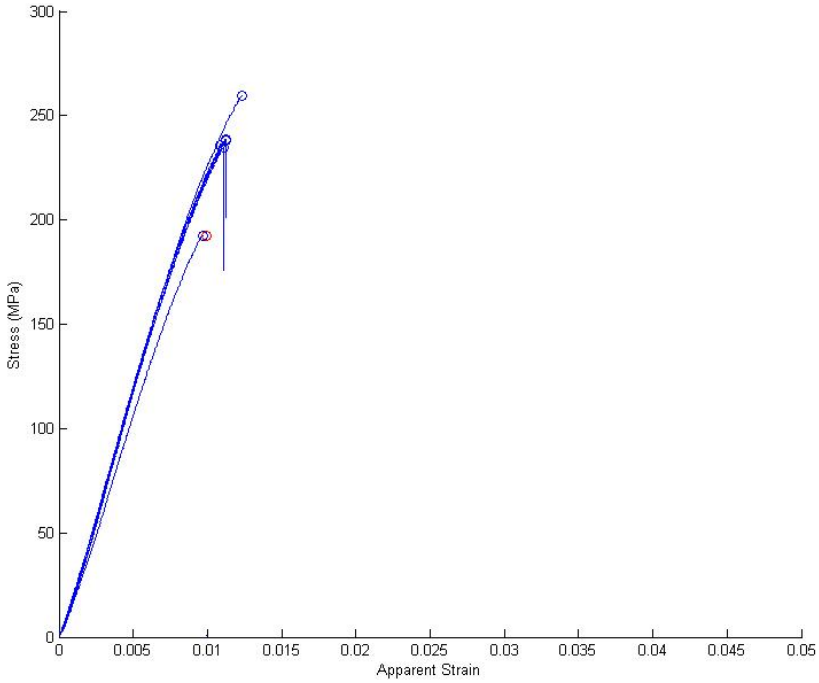

Figure 32: Stress-strain curves for samples 1-6, material B, control (no soak).

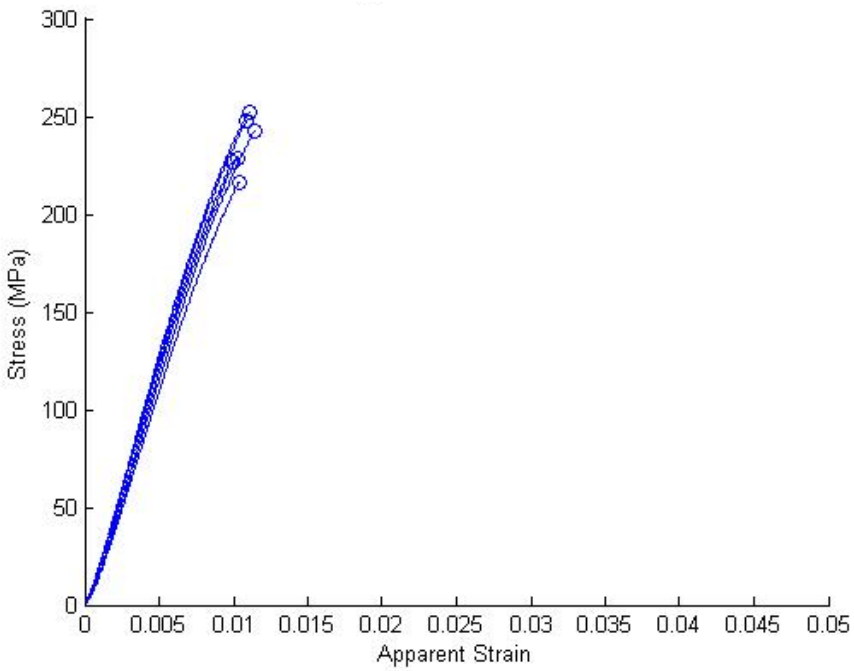

Figure 33: Stress-strain curves for samples 1-6, material B, 2-week soak.

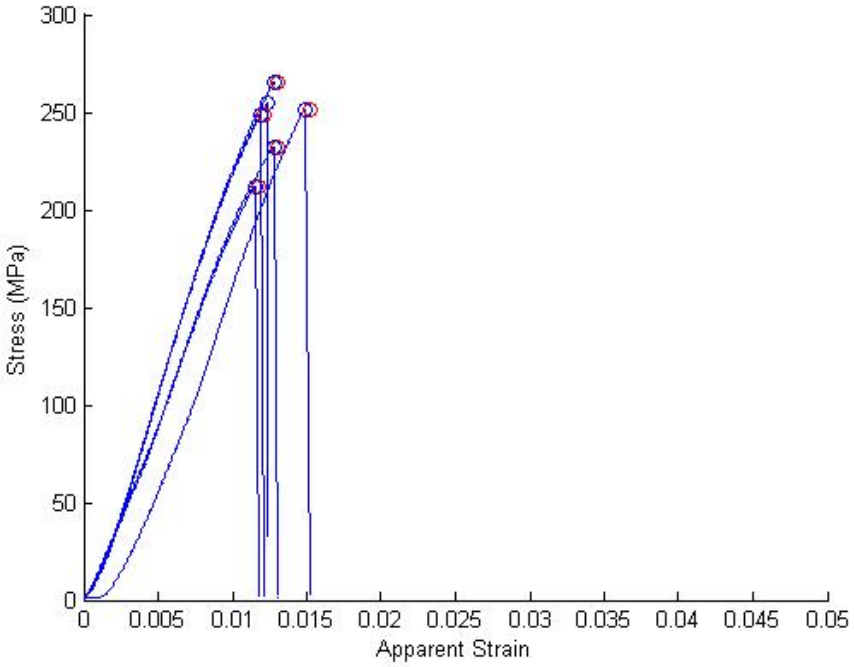

Figure 34: Stress-strain curves for samples 1-6, material B, 4-week soak.

Appendix B: Compression Test Results

Unsoaked Specimens

Block	Specimen #	Density (g/cc)	Relative Density	Moduli (MPa/mm)	Yield Stress (MPa)	Yield Strain	Ultimate Stress (MPa)	Ultimate Strain
A1	01	0.5395	0.3674	310.1059	2.8045	0.0129	3.2840	0.0184
A1	02	0.5651	0.3848	350.1610	4.0633	0.0164	4.4850	0.0208
A1	03	0.5646	0.3845	368.0340	3.3111	0.0105	3.9417	0.0167
A1	04	0.5730	0.3902	386.1537	3.6314	0.0122	4.0964	0.0164
A1	05	0.5827	0.3968	391.4112	3.4491	0.0126	3.9684	0.0169
A1	06	0.5995	0.4082	331.3309	3.4552	0.0150	3.8151	0.0193
A2	07	0.4714	0.3210	417.2679	3.9747	0.0135	4.4458	0.0174
A2	08	0.5139	0.3499	423.9712	4.7852	0.0173	xxxx	xxxx
A2	09	0.4972	0.3385	368.6948	4.7746	0.0196	5.0018	0.0217
A2	10	xxxx	xxxx	xxxx	xxxx	xxxx	xxxx	xxxx
A2	11	xxxx	xxxx	xxxx	xxxx	xxxx	xxxx	xxxx
A2	12	0.5154	0.3510	321.3769	3.2970	0.0127	3.7750	0.0168
B1	13	0.5175	0.3524	351.4952	2.9403	0.0112	3.3325	0.0159
B1	14	0.5607	0.3818	443.9464	3.8367	0.0122	4.1516	0.0153
B1	15	0.5647	0.3845	485.0531	4.5093	0.0134	5.1699	0.0181
B1	16	xxxx	xxxx	xxxx	xxxx	xxxx	xxxx	xxxx
B1	17	0.5358	0.3649	442.5382	4.0981	0.0122	4.6160	0.0161
B1	18	0.5483	0.3734	360.8043	4.0512	0.0174	4.5194	0.0224
B2	19	0.4959	0.3377	337.7469	2.8880	0.0098	3.4251	0.0162
B2	20	0.5065	0.3449	351.8545	3.5374	0.0162	4.1703	0.0224
B2	21	xxxx	xxxx	xxxx	xxxx	xxxx	xxxx	xxxx
B2	22	xxxx	xxxx	xxxx	xxxx	xxxx	xxxx	xxxx
B2	23	0.5094	0.3468	387.3430	4.3339	0.0145	5.0536	0.0216
B2	24	xxxx	xxxx	xxxx	xxxx	xxxx	xxxx	xxxx
C1	25	0.5027	0.3423	379.0373	3.8884	0.0143	4.7738	0.0231
C1	26	0.5083	0.3461	176.1854	3.0953	0.0245	3.1419	0.0261
C1	27	0.5107	0.3477	405.9856	4.2262	0.0128	4.9595	0.0189
C1	28	0.6123	0.4169	459.6421	5.1115	0.0172	5.8670	0.0233
C1	29	0.5337	0.3634	451.0694	4.6348	0.0150	5.4735	0.0214
C1	30	xxxx	xxxx	xxxx	xxxx	xxxx	xxxx	xxxx
C2	31	0.5042	0.3433	394.3854	4.1108	0.0128	4.6771	0.0183
C2	32	0.4620	0.3146	274.0547	2.9020	0.0147	3.4044	0.0215
C2	33	0.5088	0.3465	372.0576	3.7368	0.0133	4.4642	0.0208
C2	34	xxxx	xxxx	xxxx	xxxx	xxxx	xxxx	xxxx
C2	35	0.4715	0.3211	282.2911	3.4006	0.0190	3.7448	0.0232
C2	36	0.4895	0.3333	311.1221	3.4269	0.0180	3.6477	0.0220

Soaked Specimens

Block	Specimen #	Density (g/cc)	Relative Density	Moduli (MPa/mm)	Yield Stress (MPa)	Yield Strain	Ultimate Stress (MPa)	Ultimate Strain
A1	37	0.5472	0.3726	238.1477	2.3782	0.0126	2.8470	0.0199
A1	38	0.5698	0.3880	334.8426	3.0769	0.0112	3.6962	0.0186
A1	39	0.5695	0.3878	280.9843	xxxx	xxxx	xxxx	xxxx
A1	40	0.5805	0.3952	304.8788	2.6579	0.0110	3.0243	0.0157
A1	41	0.5865	0.3994	379.6056	3.9878	0.0116	5.0458	0.0223
A1	42	0.6110	0.4161	377.0846	3.8920	0.0110	4.8534	0.0207
A2	43	0.4744	0.3230	366.8751	3.2283	0.0095	3.9718	0.0174
A2	44	0.5204	0.3544	314.9993	2.8513	0.0111	3.3940	0.0169
A2	45	0.5135	0.3497	247.3658	2.8400	0.0165	3.1244	0.0202
A2	46	0.5307	0.3613	361.3993	3.7395	0.0151	4.4563	0.0227
A2	47	0.5127	0.3491	280.8650	3.1824	0.0163	3.6187	0.0220
A2	48	0.5289	0.3602	295.2235	3.3421	0.0191	3.6728	0.0213
B1	49	0.5205	0.3544	385.0380	4.3211	0.0175	5.0004	0.0215
B1	50	0.5723	0.3897	343.7718	3.4197	0.0142	4.1161	0.0191
B1	51	0.5653	0.3849	363.9018	3.4895	0.0118	4.1191	0.0185
B1	52	0.5591	0.3807	310.5448	3.3369	0.0152	3.7853	0.0210
B1	53	0.5522	0.3760	334.6434	2.9987	0.0106	3.6553	0.0187
B1	54	0.5584	0.3802	224.7749	2.3182	0.0165	2.6598	0.0213
B2	55	0.4980	0.3391	257.8295	2.1966	0.0137	2.4437	0.0175
B2	56	0.5151	0.3507	351.6345	3.1180	0.0126	3.5507	0.0177
B2	57	0.5397	0.3675	221.1649	xxxx	xxxx	xxxx	xxxx
B2	58	0.5374	0.3659	408.8715	3.6129	0.0109	4.2035	0.0165
B2	59	0.5075	0.3456	397.5680	3.6987	0.0119	4.4486	0.0191
B2	60	0.5524	0.3761	323.9168	2.7565	0.0114	3.0776	0.0157
C1	61	0.5107	0.3477	194.8132	2.3289	0.0181	2.5253	0.0215
C1	62	0.5200	0.3541	326.7922	3.4612	0.0139	4.2828	0.0234
C1	63	0.5017	0.3416	309.2971	2.8502	0.0129	3.3342	0.0187
C1	64	0.5265	0.3585	379.0142	3.3159	0.0109	3.9433	0.0161
C1	65	0.5385	0.3667	255.5572	2.7924	0.0175	3.2305	0.0242
C1	66	0.5136	0.3497	238.1191	3.0384	0.0205	3.3685	0.0250
C2	67	0.4608	0.3138	192.2773	2.8133	0.0233	3.1497	0.0289
C2	68	0.5263	0.3584	389.2599	3.9220	0.0133	4.4854	0.0182
C2	69	0.5207	0.3546	455.5252	3.5297	0.0092	4.1069	0.0143
C2	70	0.4920	0.3350	390.9220	4.3970	0.0155	5.0392	0.0214
C2	71	0.4963	0.3379	400.0621	4.1567	0.0138	4.7978	0.0190
C2	72	0.5094	0.3469	414.7445	4.0890	0.0147	4.6475	0.0193

Appendix C: Bone Screw Pullout Test Results

Dry		
Block	**Specimen #**	**Max Pullout Force** (N)
A1	1	1178
A1	2	1789
A1	3	1422
A2	4	1152
A2	5	1033
A2	6	922
B1	7	1228
B1	8	1111
B1	9	1001
B2	10	835
B2	11	1264
B2	12	1383
C1	13	1243
C1	14	1165
C1	15	1479
C2	16	1453
C2	17	987
C2	18	943

Soaked		
Block	**Specimen #**	**Max Pullout Force** (N)
A1	19	821
A1	20	875
A1	21	880
A2	22	1112
A2	23	1011
A2	24	861
B1	25	863
B1	26	924
B1	27	1217
B2	28	876
B2	29	993
B2	30	1038
C1	31	1063
C1	32	1115
C1	33	1097
C2	34	853
C2	35	1230
C2	36	789